NBS CIRCULAR 583

X-ray Attenuation Coefficients From 10 kev to 100 Mev

UNITED STATES DEPARTMENT OF COMMERCE

NATIONAL BUREAU OF STANDARDS

Data on Radiation Physics

Graphs of the Compton Energy-Angle Relationship and the Klein-Nishina Formula from 10 Kev to 500 Mev NBS Circular 542

The Compton energy versus angle relationship and the differential and integral Klein-Nishina cross sections are presented graphically as functions of the energy and direction of the scattered photon and of the recoil electron. These graphs are intended to serve the purpose of tables. Unpolarized primary gamma rays in an energy range from 10 Kev to 500 Mev are considered. The accuracy of all curves is estimated at 1 percent. The advantage of this form of presentation is the convenience and accuracy of two-way interpolation. In general, interpolated values may be obtained with an accuracy of 2 percent.

National Bureau of Standards Circular 542, 89 pages, 81 graphs. Available by purchase from the Superintendent of Documents, Government Printing Office, Washington 25, D. C., price 55 cents.

Energy Loss and Range of Electrons and Positrons

Tabulations of the mean energy loss due to ionization and excitation and the range derived from this quantity are given for electrons and positrons in several materials.

National Bureau of Standards Circular 577, 30 pages, 10 graphs. Available by purchase from the Superintendent of Documents, Government Printing Office, Washington 25, D. C., price 30 cents.

UNITED STATES DEPARTMENT OF COMMERCE • Sinclair Weeks, *Secretary*
NATIONAL BUREAU OF STANDARDS • A. V. Astin, *Director*

X-ray Attenuation Coefficients From 10 kev to 100 Mev

Gladys White Grodstein

National Bureau of Standards Circular 583

Issued April 30, 1957

For sale by the Superintendent of Documents, U. S. Government Printing Office
Washington 25, D. C. - Price 35 cents

CONTENTS

	Page
1. Introduction	1
1.1. Narrow-beam attenuation	1
1.2. Absorption and scattering processes	1
1.3. Corrections to narrow-beam measurements	2
1.4. Combination of attenuation coefficients	2
1.5. Energy absorption	3
2. Probability of processes	3
2.1. Photoelectric effect	3
2.2. Scattering by atomic electrons	5
2.3. Pair production	7
2.4. Nuclear absorption and scattering	8
3. Calculation of attenuation coefficients and comparison with experiment	9
3.1. Photoelectric effect	9
3.2. Scattering by atomic electrons	10
3.3. Pair production	11
3.4. Total attenuation coefficient	12
4. Figures and tables	13
5. Appendix	51
6. References	54

X-ray Attenuation Coefficients From 10 kev to 100 Mev*

Gladys White Grodstein

A tabulation of attenuation coefficients of X-rays and gamma rays from 0.01 to 100 Mev for 29 materials is presented. A summary of information on the probability of the basic interaction processes of photons with matter and a detailed analysis of experimental and theoretical evidence are included. Present information on the basic processes is adequate for many applications; however, improved theory and additional experimental data are needed in certain areas. A comparison of calculated and experimental coefficients points up this need.

1. Introduction

1.1. Narrow-Beam Attenuation

The attenuation coefficients tabulated here are narrow-beam, as opposed to broad-beam, coefficients. The total probability that a photon of given energy interacts with matter may be studied experimentally with a well-collimated beam of homogeneous X-rays incident upon an absorber (fig. 1). A well-shielded detector measures the intensity of the transmitted beam, and any photon absorbed or deflected appreciably does not reach the detector, if the detector is sufficiently collimated and far from the absorber. The attenuation of the intensity received by the detector as the absorber thickness is increased measures the total probability of the interaction processes. The usual semilogarithmic plot of transmitted intensity, I, versus thickness of absorber, t, follows a straight line, indicating exponential decay of the intensity according to $I(t)=I(0)\exp(-\mu t)$. The slope, μ, of the straight line represents the total attenuation coefficient, namely, the probability that a photon be removed from the incident beam per unit thickness of material traversed. A layer of matter absorbs according to the quantity of matter it contains, which is the thickness traversed times the density of the material. Therefore, absorber thicknesses are conveniently expressed on a mass basis, in grams per square centimeter. Accordingly, the attenuation coefficient is often expressed in $(g/cm^2)^{-1}=cm^2/g$ and called the mass-absorption coefficient.

1.2. Absorption and Scattering Processes

Photons may be absorbed or scattered as the result of interaction with a material. Absorption is characterized by the disappearance of a photon. Scattered photons are deflected from the original direction with or without a decrease in energy. The total probability that a process takes place per unit thickness of absorber is the sum of the probabilities of occurrence of the various absorption and scattering processes [1].[1,2] To each kind of absorption process corresponds a process of scattering; the scattering may be regarded as a combination of absorption and emission of a photon, the emission taking place in a new direction.

The most important process at low photon energy is the photoelectric effect, defined as the absorption of a photon with subsequent ejection of an atomic electron. Electrons in the K and L shells account for most of the absorption by this process at frequencies greater than the K-edge frequency; the K electrons contribute more than 80 percent of the total absorption at these frequencies. Photons with energy very much in excess of that required to eject an electron are unlikely to be absorbed. Consequently, the absorption coefficient for the photoelectric effect decreases rapidly as the photon energy increases.

Scattering of photons by atomic electrons makes a large contribution to the total attenuation coefficient in the middle energy range (0.5 to 5 Mev). Most of the scattering is incoherent, Compton scattering; a photon is deflected with a reduction in energy and an atomic electron recoils out of the atom. The probability of this process may be calculated approximately as though the atomic electrons were free. Incoherent radiation consists of a spectrum of frequencies smaller than the primary frequency. The intensity scattered in any direction is simply the sum of the intensities scattered by the individual electrons.

Some of the scattering by an atomic system is coherent, Rayleigh scattering; a photon may be deflected with no loss in energy, and the atomic system recoils as a whole under the impact. The probability of this process is large only for photons with low energy; that is, in the region where photoelectric absorption gives the main contribution to the total attenuation coefficient.

A photon with energy greater than 1 Mev may be absorbed in the neighborhood of an atomic nucleus or an atomic electron and produce an electron-positron pair. The probability for this process increases rapidly with photon energy above the threshold but levels off at higher energies. The positron of the pair is eventually annihilated with production of new X-rays. The largest fraction of the new radiation consists of photons with energy mc^2 emitted in pairs in opposite directions.

*This survey has been carried out with the support of the Biophysics Branch of the Atomic Energy Commission.

[1] Figures in bracket indicate the literature references at the end of this Circular.

[2] Reference [1] contains a classification and a qualitative description of the absorption and scattering processes.

Absorption of a photon by the atomic nucleus [2] occurs with subsequent emission of nuclear particles, mostly neutrons, and little gamma radiation. The probability of this photonuclear process has a maximum around 15 to 25 Mev, depending upon the atomic number of the absorber. In a narrow energy interval about the maximum it may give a contribution of 5 to 10 percent to the total attenuation coefficient.

Scattering of photons by atomic nuclei occurs in a manner analogous to the scattering by atomic electrons. Scattering by nuclei may be either elastic or inelastic. The probability of nuclear scattering is generally small compared to the probability of scattering by the atomic electrons. Its contribution to the total attenuation coefficient is negligible, except as noted at the end of section 2.4; it is less than 0.1 percent in the 15- to 20-Mev range for heavy elements.

Even though the contribution of these nuclear effects to the total attenuation is quite appreciable in small regions, and even though information on these effects begins to be abundant and reasonably accurate, these data do not yet constitute a body of knowledge comparable to the knowledge for electronic effects. Therefore, the main tables of this Circular include only the effects of electronic processes. Information on nuclear effects is discussed briefly in section 2.4, and some data on the nuclear contribution to attenuation are given.

1.3. Corrections to Narrow-Beam Measurements

Some radiation scattered in an absorber will always reach the detector, as seen in figure 1. The effect of receiving this scattered radiation is to increase the intensity of the transmitted beam. The intensity of singly scattered radiation can be easily calculated. If the maximum angle (θ_{max}) through which radiation is scattered into the detector is small, and if the experimental arrangement has cylindrical symmetry, the intensity of the transmitted beam is increased by the amount of scattering within a cone of aperture θ_{max}. The intensity of radiation scattered within this cone can be subtracted from the measured intensity to give the attenuation of the incident beam. For small θ_{max} the intensity of Compton scattering within the cone according to the Klein-Nishina formula is given by [3]

$$Cx\theta_{max}^2\left[1-\frac{\theta_{max}^2}{12}(9\alpha+4)\right],$$

where

x=the thickness of the absorber, in g/cm^2,

α=the incident energy, in mc^2 units, and

$$C=N\pi r_0^2\frac{Z}{A}=0.150\frac{Z}{A}\ \text{cm}^2/\text{g}.$$

[3] A similar calculation was made by Davisson and Evans [3] and by Tarrant [4], but the Tarrant paper contains an erroneous result.

There is also an appreciable amount of coherent scattering at small angles. The intensity of this radiation scattered within a cone of aperture θ_{max} can be obtained by integrating numerical data on the differential cross section for this purpose. This was done by Colgate [5], using the numerical data of Debye [6] and the equations of Franz [7];[4] see also Moon's discussion of the Franz equations [8].

The need for these theoretical corrections to the attenuation of the incident beam can be eliminated if one follows the extrapolation procedure to $\theta_{max}=0$ suggested by Colgate [5]. This procedure eliminates only the effect of Compton scattering, unless measurements are actually taken down to the very small values of θ_{max} at which coherent scattering is important.

Fluorescent radiation originating in an absorber as a result of photoelectric absorption can also reach the detector. However, the intensity intercepted by the detector in the usual narrow-beam experiment is quite small. For example, for Pb exposed to 100-kev radiation, the intensity of fluorescence per steradian is roughly 6 percent [0.95(76/100)(1/4π)] of the radiation absorbed photoelectrically. (The fluorescent yield is 0.95, and K_α radiation is isotropic with 76-kev energy.) Assuming for the detector aperture a solid angle of 0.01 steradian, which is rather large for this type of experiment, the measured intensity of the 76-Kev radiation is roughly 0.06 percent of the intensity absorbed photoelectrically from the incident 100-kev radiation.

The number of annihilation photons from the absorber that reach the detector will be similarly small in the usual narrow-beam experiment. Assuming that all radiation emitted is from 2 quanta annihilation and is isotropic, the number of photons per steradian will be approximately 16 percent of the number of pairs produced. The number of photons detected in a solid angle of 0.01 steradian is only 0.16 percent of the number of electron-positron pairs produced in the absorber by the incident radiation.

1.4. Combination of Attenuation Coefficients

The probabilities of interaction processes of an X-ray photon with different atoms of an absorber add up without mutual disturbance, in general. The effect of chemical binding on the interaction of X-rays with valence electrons is exceedingly weak. However, the orderly arrangement of atoms next to one another does influence the total probability of interaction processes to an extent that is quite considerable, expecially in Bragg reflection by crystal lattices, when the momentum transfer from photon to matter is of the order of the Planck constant divided by the spacing of adjacent atoms. Special situations of this kind are disregarded in the present Circular. Within this approximation, the mass-attenuation

[4] The total cross section of Franz is too small by a factor of 2 owing to an analytical error.

coefficient of a chemical compound or mixture is an average of the mass attenuation coefficients of the constituent elements, weighted in proportion to the abundance of each element by weight. For example, for water (1 part H, 8 parts O), we have $\mu_{H_2O}=(1/9)\mu_H+(8/9)\mu_O$, provided the μ's are expressed as mass-attenuation coefficients.

1.5. Energy Absorption

Most of the energy transferred from X-rays and gamma rays to a material is given to electrons or positrons and then dissipated along the path of these particles. Part of this energy is absorbed by inelastic collisions with other atomic electrons and some is released to photons of lower energy. Thus the energy of the incident photon is not entirely absorbed at the point of its interaction in the material. In fact, at energies greater than a few million electron volts, electrons may travel distances comparable to the mean free path of photons of the same energy. There are problems, as in dosimetry and in medical or biological studies, that require a calculation of the probable energy transfer to a material by a beam of X-rays. The fraction of energy dissipated locally by a narrow beam of X-rays is given by the product of the probability of each interaction process and the probable fraction of the photon energy that is dissipated locally in the absorber as a result of the process. The definition of the term "locally" is not unique; it will depend on the energy of the incident radiation, on the material of the absorber, and further on the purpose of a particular measurement and the viewpoint of the observer.

2. Probability of Processes

Theoretical methods for calculating the probability of the basic interaction processes of photons with matter are well established. However, systematic calculations are complicated. Various kinds of approximations can be utilized, but their proper application requires some care. Substantial uncertainty still exists regarding many details of the approximation procedures.

Nevertheless, theory has progressed to the point where the present tabulation of data has been derived primarily from theory, with experimental data providing the necessary checks and some additional fitting.

2.1. Photoelectric Effect

The probability of the photoelectric effect [5] exhibits, as main features, a very rapid decrease as the frequency of the incident X-ray increases and a rapid increase as the atomic number of the material increases. This behavior appears natural because an electron can resonate under the driving action of a high-frequency disturbance only if it is held by a very strong force such as obtains in the space immediately surrounding an atomic nucleus. This portion of the atomic volume, where the force is adequate, is a decreasing function of the driving frequency and an increasing function of the magnitude of the nuclear charge. When the photon energy $h\nu$ exceeds mc^2 most of the momentum of the ejected electron is imparted directly by the incident photon. The attraction by the nucleus need supply only a momentum of the order of mc, no matter how large is the energy $h\nu$. Accordingly, the probability of the photoelectric effect decreases more slowly as the energy $h\nu$ keeps increasing in the relativistic range.

Simplifying assumptions. The main approximations that are usually considered in any theoretical analysis of the photoelectric effect involve one or more of the following features:

(a) Schematic treatment of the interaction among atomic electrons, in the form of "screening effects," which permits the use of hydrogen-like wave functions for the atomic electrons.

(b) Treatment of the electron motion according to nonrelativistic quantum mechanics (valid for $h\nu/mc^2<<1$, $(Z/137)^2<<1$).

(c) Disregard of the attraction exerted by the nucleus on the electron as it leaves the atom (Born approximation valid for $Z/(137v/c)<<1$, where v is the speed of the ejected electron).

(d) Disregard of the possibility that the ejected electron may receive from the radiation an angular momentum larger than $h/2\pi$ (dipole transition approximation). This assumption is justified if the X-ray wavelength is much larger than the initial wavelength of the atomic electron.

(e) Treatment of the electron motion by the Sommerfeld-Maue-Furry approximation (angular momentum quantum number $j>>Z/137$). This approximation is useful when the conditions are opposite to (d), that is, when (at very high energies) most of the photoelectric effect is contributed by high order multipoles.[6]

The interaction of radiation with the atomic electron is normally treated as "weak." Higher-order electrodynamic effects require corrections of the order of 1/137 or smaller.

As a further approximation, one often assumes that the probability ratio of photoelectric ejection of different electrons is energy independent in the range of interest. Because this approximation is reasonable, and as K electrons have the largest chance of being ejected by X-rays above the K edge, most data in the literature deal with the photoelectric effect in the K shell.

The principal calculations which have been

[5] See Sommerfeld [9] and Hall [10] for reviews of the theory of the photoelectric effect.

[6] Bethe and Maximon [11] used this approximation in the calculation of the differential cross section for bremsstrahlung and pair production.

carried out in detail are listed below, with an indication of the pertinent approximations.

Simple Born calculation (approximations a, b, c). The cross section for photoelectric effect in the K shell of an atom with atomic number Z for a photon of energy $h\nu$ is [12, p. 207]

$$\sigma_K=\phi_0 4\sqrt{2}\left(\frac{mc^2}{h\nu}\right)^{7/2}\frac{Z^5}{137^4};\quad \phi_0=\frac{8}{3}\pi r_0^2. \tag{1}$$

Sauter formula (approximations a, c). The corresponding relativistic calculation was made by Sauter [13]. The assumption (b) is thereby eliminated.

Stobbe formulas (approximations a, b, d). A basic calculation, using exact nonrelativistic hydrogen-like wave functions, was made by Stobbe [14] for electrons of the K, L, and M shells. Its results can be expressed by a factor f [12], which represents the ratio of the "non-Born" cross section to the "Born" cross section eq (1).

Sauter-Stobbe combined formula. The Sauter-Born approximation cross section may be corrected to a considerable extent by multiplying it with the factor f derived by Stobbe under a nonrelativistic approximation. The combined formula becomes

$$\sigma_K=\frac{3}{2}\phi_0\frac{Z^5}{(137)^4}\left(\frac{mc^2}{h\nu}\right)^5(\gamma^2-1)^{3/2}\left[\frac{4}{3}+\frac{\gamma(\gamma-2)}{\gamma+1}\times\left(1-\frac{1}{2\gamma\sqrt{\gamma^2-1}}\ln\frac{\gamma+\sqrt{\gamma^2-1}}{\gamma-\sqrt{\gamma^2-1}}\right)\right]\left[2\pi\sqrt{\frac{I}{h\nu}}\frac{e^{-4x\,\mathrm{arc\,cot}\,x}}{1-e^{-2\pi x}}\right] \tag{2}$$

where

$$\gamma=\frac{h\nu}{mc^2}+1,\ x=\sqrt{\frac{I}{h\nu-I}},\ \text{and } I=(Z-0.3)^2\ Ry.$$

Hulme calculation (approximation a). A calculation using exact relativistic hydrogen-like wave functions was made by Hulme [15]. The results are given numerically for a few values of the atomic number and of the photon energy. Interpolation is possible to a considerable extent. Approximation (d) is set aside, but the requirement to carry out the calculations for many successive terms of the dipole, quadrupole, . . . sequence makes the procedure prohibitively laborious at $h\nu/mc^2>>1$.

Hall formula (approximation a, $h\nu/mc^2>>1$). Hall [16, 10] developed a high-energy formula that does not rely on the Born approximation, like the Sauter formula, or on a separate evaluation of the dipole, quadrupole, . . . sequence, like the Hulme calculations. Hall gives

$$\sigma_K=\frac{3}{2}\phi_0\frac{Z^5}{137^4}\frac{mc^2}{h\nu}Re^{-\pi\alpha+2\alpha^2-2\alpha^2\ln\alpha} \tag{3}$$

where

$$R=1+[4(1-\alpha^2)^{1/2}-5/3]\frac{mc^2}{h\nu},\ \text{and } \alpha=Z/137.$$

Nagasaka formula (approximations a and e). Nagasaka [17] developed a high-energy formula, using the Sommerfeld-Maue function for the final state and the exact Dirac wave function for the initial state of the K-electron. The Sommerfeld-Maue function may be used for the final state of the electron in the photoelectric effect so long as $(Z/137)^2(\epsilon^{-1}\ln\epsilon)<<1$, where ϵ is the energy of the electron in units of mc^2. The effect of screening was completely neglected in this calculation, which is justified by the remark in footnote 7.

Nagasaka's cross section has the form

$$\sigma_K=\frac{3}{2}\phi_0\frac{Z^5}{137^4}\frac{mc^2}{h\nu}G\left[\sigma_0-\sqrt{\epsilon\frac{mc^2}{h\nu}}\frac{\epsilon-2}{\epsilon-1}0.832\frac{Z}{137}+1.476\frac{Z^2}{137^2}\right], \tag{4}$$

where $\epsilon=1+(h\nu-I)/mc^2$ is the total energy of the ejected electron (including its rest mass) in units of mc^2, G is a factor discussed below, and

$$\sigma_0=\frac{(\epsilon^2-1)^{3/2}}{(\epsilon-1)^4}\left[\frac{4}{3}+\frac{\epsilon(\epsilon-2)}{\epsilon+1}\left(1-\frac{1}{2\epsilon\sqrt{\epsilon^2-1}}\ln\frac{\epsilon+\sqrt{\epsilon^2-1}}{\epsilon-\sqrt{\epsilon^2-1}}\right)\right]. \tag{5}$$

Notice that eq (4) reduces to the Sauter formula (2) if the terms following σ_0 are disregarded; G is taken as 1, and I is disregarded in the definition of ϵ, so that $\epsilon=\gamma$. In the high-energy limit, more specifically for $1/\epsilon^2<<1$, Nagasaka finds

$$G=\exp\,[-\pi Z/137+2(Z/137)^2-(Z/137)^2\ln\,(Z/137)]. \tag{6}$$

The corresponding factor in Hall's formula (3) has an additional factor of 2 in front of the logarithm in the exponent. The Hall and Nagasaka calculations differ in formal procedure but utilize in fact the same approximation. Part of the difference between the results (3) and (4) has been traced by Nagasaka to an algebraic mistake in Hall's calculation.

Most calculations in the literature deal with the photoelectric absorption in the K shell, which greatly exceeds the absorption in other shells for X-ray energies above the K edge. For energies well above the K edge, absorption in the L_{I}, M_{I}, . . . subshells greatly exceeds the absorption in the L_{II}, L_{III}, M_{II}, . . . subshells, because electrons with azimuthal quantum number $l=1, 2$, . . . are kept away from the proximity of the nucleus by centrifugal action, and therefore, experience less attraction than $l=0$ electrons. The relative probability of photoelectric effect in the K, L_{I}, M_{I}, . . . subshells should be approximately independent of the photon energy at high energies, according to elementary theory. These prob-

abilities should be approximately in the same ratios, 1, $1/2^3$, $1/3^3$, . . . as the probabilities that K, L_1, M_1, . . . electrons be near the nucleus. The Stobbe formulas indicate a slight decrease of the ratios of L to K, M to K, . . . as $h\nu$ increases. An application of the Hall formula to a calculation of σ_L/σ_K at 2.62 Mev for Pb yields 0.20, which is considerably more than one-eighth. Limited experimental evidence has indicated [18], as an approximate rule, that the total probability of photoelectric effect at high energies equals 5/4 of the probability for the K shell alone. Notice that 5/4 is a little larger than the sum $1+1/2^3+1/3^3=1.16$.

A simplified treatment of the interaction among atomic electrons (approximation a) may suffice for the photoelectric action on K shell electrons for which nuclear attraction greatly predominates over other attractions. The portion of the electronic cloud that lies nearer to the nucleus than the photoelectron effectively offsets, or "screens," the nuclear charge to some extent. This effect may be taken into account by attributing to the nucleus an "effective atomic number" $Z-s$. The number s, called the "inner screening number," was evaluated semiempirically for the electrons of the various shells by Slater [19]; values of s are given in table 1.[7]

The portion of the electronic cloud, that is farther away from the nucleus than the initial position of the photoelectron, affects this electron like an "outer screening," that is, like an external electrically charged shell. This shell does not exert any electric force upon a charge inside, where the photoelectron is, but establishes a negative potential difference of V_0 volts between the interior of the shell and external points at infinite distance. The effect of this potential energy becomes apparent when the electron escapes from the atom. As soon as the electron reaches the outside of this shell the charge of the shell exerts a repulsive force and thus helps the escape from the nuclear attraction. The effective value of V_0 may be determined by observing that the experimental value of the initial binding energy of the photoelectron is eV_0 ev smaller than the energy pertaining to a hydrogenlike wave function with effective atomic number $Z-s$.

On this basis, the absorption of a photon with energy $h\nu$ by an atomic electron appears to take place inside the outer screening shell under the influence of attraction by a nuclear charge $(Z-s)e$. The outer screening does not influence the process of absorption or the probability of the subsequent ejection of the electron from the atom.[8] The hydrogenlike wave functions of the electron within the atom before and after absorption of the photon correspond to energy levels evaluated as though the outer screening were absent. (The energy of the ejected electron may become negative when reduced by eV_0, if $h\nu$ is only a little above the absorption edge. This circumstance introduces no real difficulty because formulas for the hydrogenlike approximation carry over to negative values of the energy.)

[7] Bethe has pointed out (in a private discussion) that when photoelectric effect takes place near the nucleus, well inside the K shell, the inner screening effect should vanish. Accordingly, it may be inappropriate to utilize an inner screening number $s>0$ whenever the photon energy is greatly in excess of the K absorption edge. This remark probably explains why the probabilities of photoelectric effect calculated with $s=0.3$ for low-Z elements are substantially lower than indicated by experimental evidence and had to be modified by an empirical correction, as discussed in section 3.1.

[8] This probability would be influenced only if the outer screening potential varied rapidly from point to point, which is not the case (see M. E. Rose, Phys. Rev. 48, 727 (1936)). The calculation by Hall [10, p. 283] of a correction to the cross section of the photoelectric effect arising from outer screening appears to be inconsistent with his application of a WKB approximation.

2.2. Scattering by Atomic Electrons

The main contribution of scattering to the total attentuation coefficient arises from simple Compton effect processes [9] in which the bonds of the atomic electrons within the material can be disregarded. More complex scattering conditions obtain at the lower photon energies where photoelectric absorption predominates over the attenuation due to scattering. Therefore, these more complex effects, which include coherent Rayleigh scattering, do not influence the over-all attenuation very greatly.

The Compton scattering by "free" electrons is described to a very good approximation by the theoretical Klein-Nishina law. Corrections arising from higher-order electrodynamic effects have been calculated and amount to about 1 percent only. Experimental evidence agrees well with the Klein-Nishina value of the scattering cross section by free electrons, in the energy region where Compton scattering gives the main contribution to total attenuation. The differential cross section for scattering of a photon of frequency ν, with a deflection θ into a solid angle $d\Omega$, is

$$d\sigma(\theta)=\frac{r_0^2}{2}\frac{1}{[1+\alpha(1-\cos\theta)]^2}\left\{1+\cos^2\theta+\frac{\alpha^2(1-\cos\theta)^2}{1+\alpha(1-\cos\theta)}\right\}d\Omega, \tag{7}$$

where $r_0^2=(e^2/mc^2)^2=7.94\times10^{-26}cm^2$, $\alpha=h\nu/mc^2$, and h, m, and c have the usual meaning. The integral cross section is

$$\sigma_{K-N}=2\pi r_0^2\left\{\frac{1+\alpha}{\alpha^3}\left[\frac{2\alpha(1+\alpha)}{1+2\alpha}-\ln(1+2\alpha)\right]+\frac{\ln(1+2\alpha)}{2\alpha}-\frac{1+3\alpha}{(1+2\alpha)^2}\right\}. \tag{8}$$

For $\alpha<<1$ [21], the following formula is convenient,

$$\sigma_{K-N}=\phi_0[1-2\alpha+5.2\alpha^2-13.3\alpha^3+32.7\alpha^4\ldots]. \tag{9}$$

The integral cross section (8) is tabulated in table 2.

[9] For a fuller discussion of Compton scattering and extensive tabulations of the Klein-Nishina formula, see Nelms [20].

The assumption of free electrons that underlies the Klein-Nishina formula holds only if the momentum transferred to the electron greatly exceeds the initial momentum of the electron's motion within an atom or molecule. In terms of the initial wavelength of the radiation (λ) and of the atomic electron λ_{at} this condition reads

$$\frac{\lambda}{2\sin(\theta/2)} << \lambda_{at}$$

and obtains less frequently than one may be inclined to expect.

When this condition does not obtain, Compton scattering is complicated by the bonds that hold the atomic electrons and becomes less frequent than predicted by the Klein-Nishina law. The decrease of incoherent (inelastic) Compton scattering is accompanied by an increase of coherent scattering [10] in which the photon loses no energy. As a result of constructive interference of the radiation scattered coherently by different electrons, the *total* cross section for scattering of lower-energy photons grows larger than predicted by the Klein-Nishina formula.

In an approximate calculation, one may regard the probability of Compton scattering by an atomic electron as the product of two factors. The first factor concerns the probability that the photon be deflected by a certain angle and transfers to the electron a corresponding amount of momentum q *as though* the electron were free. The momentum transfer is given by $q \sim (h\nu/c) \times 2\sin(\theta/2)$ for $h\nu(1-\cos\theta) << mc^2$. The second factor concerns the probability that the electron, having received a momentum q, will actually absorb energy and thereby become excited or leave the atom. This analysis of probability into two factors derives from the impulsive character of the scattering process.[11]

For the first factor one may take the Klein-Nishina cross section (8) for free electrons. For the second factor one may take the incoherent scattering function $S(q,Z)$ which is discussed in some detail in the appendix. If q is much smaller than the root mean square momentum of the electron before the scattering, the second factor S becomes very small in proportion to 1 and any actual energy transfer is comparable to the binding energy of the atomic electron. If q is much larger than the initial rms momentum, S equals approximately 1, and the actual energy transfers are in a narrow band about $q^2/2m$. Thus incoherently scattered radiation disappears at very low energies and approaches the value given by the Klein-Nishina formula at high energies. The total cross section for incoherent scattering with deflection θ by the Z electrons of an atom equals approximately

$$d\sigma_{\text{incoh}} = (1/2)Zr_0^2[1+(h\nu/mc^2)(1-\cos\theta)]^{-2}\{1+\cos^2\theta + (h\nu/mc^2)^2(1-\cos\theta)^2/[1+(h\nu/mc^2) \times (1-\cos\theta)]\} S(q,Z)d\Omega. \quad (10)$$

To calculate the probability of *coherent* Rayleigh scattering one must combine the amplitudes rather than the intensities corresponding to scattering with a given momentum transfer to the different electrons. Here again the probability results as the sum of two factors. The first factor follows from the Klein-Nishina formula (7) by deleting (a) the last term in the braces, which corresponds to a flipping of an electron spin and is inconsistent with coherent scattering, and (b) the factor $[1+(h\nu/mc^2)(1-\cos\theta)]^{-2}$, which arises from the ratio of the incident and scattered frequencies and must equal 1 for coherent scattering. The second factor of the coherent scattering cross section is somewhat complementary to the incoherent scattering function S, in that it represents the probability, $|F(q,Z)|^2$, that the Z electrons of an atom take up a recoil momentum, q, without absorbing any energy. The function $F(q,Z)$ is called the form factor. The cross section for coherent scattering equals:

$$d\sigma_{\text{coh}} = (1/2)r_0^2(1+\cos^2\theta)|F(q,Z)|^2 d\Omega. \quad (11)$$

The form factor F and the cross section (11) are usually calculated separately for each kind of atom in a material. This procedure was indicated in section 1.4 as generally adequate, with exceptions. Additional scattering may actually arise from interference among the X-rays scattered coherently by electrons of different atoms. This effect depends on the state of aggregation of adjacent atoms. Its order of magnitude may be lower than or comparable to the effect of interference of electrons from the same atom for polyatomic gases, liquids, or amorphous solids. It becomes extremely large for crystalline solids under conditions of Bragg reflection. To calculate this effect one must define and evaluate a suitable scattering factor F, which depends on the arrangement of atoms of the material.

The cross sections (10) and (11) are derived under the restrictive assumption that the X-ray frequency is much larger than the proper oscillation frequencies of atomic electrons, i. e., that the photon energy greatly exceeds the energies at which photoelectric absorption is intense. Insofar as this assumption is not fulfilled, the coherent scattering cross section depends more critically on the ratio between the X-ray frequency and the proper frequencies of the electrons (effect of anomalous dispersion). However, the assumption fails seriously just at those energies where the

[10] For a fuller discussion of coherent scattering and tabulations of form factor data, see Nelms and Oppenheim [22].

[11] The momentum transfer takes place, in the main, in a time short as compared to the reaction time of the mechanism that binds the electron in the atom. Thus the determination of momentum transfer and angular deflection occurs in a much shorter time than the determination of the energy transfer. The former depends on the photon-electron interaction, the second on the electron-atom interaction.

photoelectric cross section is much larger than the scattering cross section. Therefore, an accurate knowledge of scattering is not required for acceptable accuracy on the total probability of interactions. The progress towards improved calculations of coherent scattering is discussed in [22]. The Rayleigh scattering by electrons combines coherently with other processes of elastic scattering, such as Delbrück scattering and elastic nuclear scattering; however, this interference effect is of importance only for large photon energies and scattering angles at which all of these processes together yield a negligible contribution to the total attenuation coefficient.

2.3. Pair Production

The production of an electron-positron pair by the absorption of a photon may be regarded as a photoelectric effect with the ejection of electrons from negative energy states. Calculation of the pair production probability is, therefore, analogous to the photoelectric calculation. The pertinent approximations are of the same types except for two main differences; (a) pair production occurs only at relativistic energies (approximation (b) of section 2.1 is never valid) and (b) the initial state of the electron belongs to a continuum for pair production and to a discrete spectrum for the photoelectric effect.

The principal calculations that have been carried out in detail for the production of an electron-positron pair in the field of the nucleus are listed below with an indication of the pertinent approximations.

Born calculation (approximations a and c). The differential cross section was calculated for pair production in the Coulomb field of the nucleus by Bethe and Heitler [23] and concurrently by Sauter [24] and Racah [25].[13] The effect of screening of the nuclear field by the atomic electrons was studied by Bethe [26]. In Born approximation the screening effect consists of a destructive interference of the field of the atomic electrons with the nuclear field. This interference reduces the cross section by a factor $[1-F(q,Z)]$,[2] where $F(q,Z)$ is the same atomic-form factor that describes coherent scattering of X-rays; that is, the probability amplitude that the atomic electrons absorb a momentum q without absorbing any energy. Bethe and Heitler calculated screening functions for a Fermi-Thomas distribution of electrons. Analytical integration over the possible values of recoil momentum given to the atom is possible only for the limiting cases of complete or no screening; numerical integration must be performed for the cases of incomplete screening. The necessary formulas and numerical data are given, e. g., [2, p. 260].

Wheeler and Lamb [27] calculated screening functions for hydrogen using atomic wave functions. A comparison of the cross sections for atomic hydrogen in the case of complete screening shows the Wheeler-Lamb value to be approximately 2 percent above the Fermi-Thomas result.

Non-Born calculation for low energy (approximation a). A calculation using exact relativistic wave functions for an electron in an unscreened nuclear field was made by Jaeger and Hulme [28] and Jaeger [29]. They obtained numerical results for photon energies of 3 and 5.2 mc^2 and for a few elements; some interpolation of their results is possible. For Pb at 3 mc^2 the Born approximation value is lower by a factor of about 2 than the Jaeger-Hulme value; the difference is much smaller at higher photon energy and lower atomic number.

Non-Born calculation for high energy (approximations a and e). The cross section for specified energy and direction of each particle of the pair was calculated by Bethe and Maximon [11] without the use of Born approximation for energies large compared to mc^2. The total cross section was obtained by analytical integration by Davies, Bethe, and Maximon [30]. The correction to the Born approximation calculation is important only for large momentum transfer to the atom where screening is not important; therefore, this correction may be applied equally to the cases of complete, incomplete, or no screening. For the practical cases of incomplete screening a correction (calculated in reference 11 and approximately proportional to Z^2) may simply be subtracted from the screened Born approximation calculation to give the total cross section. For photon energy $\epsilon=h\nu/mc^2$ the main residual error in the calculations of reference 30 is known to be of the form $(a^2 \log \epsilon)/\epsilon$, where a^2 can be determined by fitting to the experimental data for each element.

Pair production in the electron field. Pair production necessarily imparts a recoil momentum to the electric field in which it takes place. The calculations indicated above pertain to the case where the recoil is absorbed by an atom as a whole; the electrons remain rigidly attached to the nucleus so that their fields combine coherently with the nuclear field to yield a screening effect. In addition, the recoil may be absorbed by a single atomic electron which is thereby ejected from the atom. The total cross section for this process results as the sum of the incoherent contributions from all electrons. The recoiling electron can take up a substantial fraction of the energy of the incident photon but this occurs mainly for photon energies near the threshold; the threshold here is 4 mc^2 instead of 2 mc^2.

Calculation without exchange (approximation c). This calculation was made by Borsellino [31], assuming the electron to be free from atomic bonds. The cross section was integrated analytically over the energies and directions of the pair particles for photon energies from 4 to 100 mc^2. In this calculation the total cross section for the electron field approaches that of an unscreened

[13] For a discussion of the angular distributions in electron-positron pair and bremsstrahlung production see, H. Brysk (informal communication).

H atom as the photon energy becomes much larger than mc^2.

In order to take into account the bonds of electrons within atoms, the cross section for pair production with a given recoil of a free electron must be multiplied by the probability that this recoil actually ejects an electron from its atom. This probability is the same incoherent scattering function $S(q,Z)$ that appears in (10) and is discussed in the appendix. The cross section thus reduced must then be integrated over all possible values of the recoil momentum.

A calculation of this type was made by Wheeler and Lamb [27], using the incoherent scattering function derived from the Thomas-Fermi model. The total cross section was obtained by integrating only over momentum transfers up to mc for incident photons with energies large compared to mc^2. The Thomas-Fermi model gives an erroneously large probability of incoherent scattering for small values of the recoil momentum. This fact is borne out in the comparison Wheeler and Lamb made between a calculation using the Thomas-Fermi model and a similar calculation using atomic wave functions for hydrogen; for photon energies very large compared to mc^2 the two calculations differ by approximately 12 percent.

Calculation with exchange (approximation c). This calculation was made by Vortruba [32] for an electron free of atomic bonds. An integral cross section was obtained only for the limiting cases of photon energy near the threshold or large compared to mc^2 and yielded the approximate formulas [13]

$$\sigma_{\text{Pair}}=5.6\times10^{-3}\frac{r_0^2}{137}\left(\frac{h\nu}{mc^2}-4\right)^2 \quad \text{for } 0\leq\frac{h\nu}{mc^2}-4\lesssim 1 \tag{12}$$

$$\sigma_{\text{Pair}}=\frac{r_0^2}{137}\left(\frac{28}{9}\ln\frac{2h\nu}{mc^2}-11.3\pm0.5\right) \quad \text{for } \frac{h\nu}{mc^2}>>1 \tag{13}$$

with $r_0^2=7.94\times10^{-26}\,\text{cm}^2$.

The exchange effect (due to the identity of the recoil and pair electron) is very large near the threshold energy; a factor of 4.5 between the results of Borsellino and Vortruba is attributed to this effect. The effect of exchange decreases greatly when the recoil electron takes up very little of the available energy. This situation predominates when the photon energy is large compared to mc^2. Therefore, it was believed that the Borsellino calculation would be adequate in this region. However, the detailed recalculation by Rohrlich and Joseph [33] shows that the difference between the cross sections of Vortruba and Borsellino is quite substantial; the former is only about 75 percent of the latter at a photon energy of 100 Mev.

A calculation by Rohrlich and Joseph [33] for atomic hydrogen in the limit of photon energy very large compared to mc^2 shows that the exchange effect modifies the result of the Wheeler-Lamb hydrogen calculation by about 19 percent.[14] Exchange weights the momentum transfer distribution toward smaller momenta and therefore decreases the cross section for pair production with electron recoil. (The cross section for pair production with nuclear recoil is increased slightly.)

Other calculations of the cross section in the electron field were made by Nemirovsky [35] and Watson [36]. Nemirovsky was concerned only with a photon energy near the threshold, and his numerical result is essentially in agreement with Vortruba. Watson obtained a cross section that approaches twice that of an unscreened H atom as the photon energy becomes very large compared with mc^2.

2.4. Nuclear Absorption and Scattering

The absorption of a photon with subsequent emission of nuclear particles (nuclear photoeffect) makes a contribution to the total attenuation coefficient that is usually of the order of 5 percent or less and confined mainly to an energy interval of less than 10 Mev, but is occasionally substantially larger. No data on nuclear absorption are given in the main tables of this Circular, but some information on the process is given and is utilized for the analysis of experimental data in the region where this process is comparatively important.

The probability of the nuclear photoeffect has the following main trend. It increases rapidly with energy above the threshold for emission of nuclear particles, reaches a maximum and then decreases rapidly as the energy of the incident photon increases further. The position of maximum cross section varies from about 13 Mev in uranium to about 23 Mev in carbon. The width of the absorption curve appears to show no systematic variation but varies from 5 to 8 Mev. Values of the cross section for neutron emission in this broad maximum vary with atomic weight from about 10 millibarns in carbon to 1 barn in uranium [37, 38]. A cross section of the same order of magnitude is estimated for proton as for neutron emission from low-Z nuclei.

Cross sections for photoneutron emission are given in table 3 for comparison with total cross

[13] An exact evaluation by Rohrlich and Joseph [33] of the constant in this equation gives 11.78 instead of 11.3±0.5.

[14] An experiment by Bernstein and Panofsky [34] indicates that exchange effects are not negligible at very high photon energies in the production of bremsstrahlung, which is closely related to pair production. The production of 235-Mev photons by 500- and 550-Mev electrons in liquid hydrogen was measured and compared with the Wheeler and Lamb calculations; the measured result was 2.4±2.8 percent below the calculated value. An increase of about 3 percent in the measured value above the calculation is expected due to interference effects between the individual nuclei and electrons in the hydrogen molecule, whereas a decrease is expected because of neglect of exchange effects in the calculation. The magnitude of this decrease can be inferred from the calculations of Rohrlich and Joseph, who find for atomic hydrogen in the very high energy limit that the total integral cross section for pair production (sum of values in the nuclear and the electron field) is decreased by about 9 percent by the exchange effect.

sections for non-nuclear processes tabulated in this circular. The data for the photonuclear effect from Katz [15] et al. were plotted and values were read from a smooth curve over the interval for which the cross section is about 1 percent or more of the total absorption cross section. The interval covers 5 to 8 Mev, and the photoneutron cross section at maximum is 4 or 5 percent of the total absorption cross section.

Data on the elastic scattering of X-rays [39] associated with the nuclear photoeffect show the same general features as the neutron yield data. The maximum cross section varies from 0.12 millibarn for Na to 15 millibarns for Pb. These cross sections are about 100 times smaller than the corresponding values from neutron yield data and are negligible compared to the total attenuation coefficient.

X-rays can also be absorbed or scattered by nuclei with high probability, if their frequency lies within certain narrow resonance lines. These lines lie at lower energy than the main continuous absorption spectrum, mostly near to or below the threshold for particle disintegration. The photon energy corresponding to individual lines is known only in few instances. The width of typical lines is of the order of 1 ev. The aggregate absorption of the line spectrum from a continuous spectrum of X-rays is negligible, but for X-rays within the line width the cross section probably often approaches a theoretical limit of the order of 100 barns.

3. Calculation of Attenuation Coefficients and Comparison With Experiment

The data tabulated in tables 12 to 40 were derived primarily from theoretical calculations. Experimental data served primarily as a check, but also as a guide in settling dubious questions and providing empirical corrections.

3.1. Photoelectric Effect

The cross section for the photoeffect in the K shell was calculated by the Sauter-Stobbe formula (2) in the low-energy range. Correction factors in table 4 were applied to the Sauter-Stobbe formula at energies from 10 to 100 kev (see discussion below). In the energy range between 0.34 and 1.1 Mev interpolated data from the Hulme calculations (see p. 4) were utilized. In the high-energy region the Hall formula for $h\nu \gg mc^2$ (3) was used. An effective nuclear charge of $Z-0.3$ was used throughout to correct for screening in the K shell (see p. 5).

Cross sections for the L and M shells were calculated by the Stobbe formulas.[16] Above the K edge lengthy calculations for the L and M shells were avoided by a procedure that relies on the slowness of variation of the ratios among the cross sections for different shells. The ratios given by the Stobbe formulas were calculated at the K edge and at an energy of 340 kev. These ratios are given in table 5 for a number of elements.[17]

The Sauter-Stobbe calculations, which serve as a zero approximation to the K shell cross section throughout the interval from the K edge to 340 kev, were corrected for the effect of the L and M shells on the basis of the ratio at the K edge. The other two calculations, from Hulme and from the Hall formula, were corrected initially on the basis of the ratio at 340 kev.

The three sets of values so obtained were then plotted together and graphical adjustment was made by drawing a smooth curve which represents the final photoeffect cross section. Figures 2 and 3 illustrate the procedure followed and show comparisons with both theoretical and experimental data. Only a limited revision of the analysis based on Hall's calculation was required by Nagasaka's results indicated on p. 4.

Discussion of data for $h\nu > 1$ Mev. Comparison of calculations by the Hall formula (3) and the Nagasaka formula (4) is shown in figure 2. The calculations agree within 1 percent at $h\nu = 2.6$ Mev, which is approximately the crossover point of the two calculations. The Hall data at 2.6 Mev was used to interpolate from the Hulme data at 1.1 Mev into the high-energy region. The errors in Hall's formula will affect the photoeffect cross sections tabulated in this report above about 3 Mev for Pb; the resulting uncertainty in the total cross section is not significant.

Latyshev [18] made the only direct measurement of photoeffect cross section in the high-energy region. Other data shown in figure 2 was obtained from measurements of the total cross section by subtracting the scattering (coherent and incoherent) and pair production cross sections. The errors indicated on each point correspond to the error quoted by the author for the total cross section. The only data showing significant deviation from the calculated curves are the values at 2.62 Mev ($\lambda \sim 0.2$) and at 5.3 Mev ($\lambda \sim 0.1$).

Discussion of the data for $h\nu$ between 0.1 and 1 Mev. The experimental data shown in figure 3 were obtained by subtracting the scattering cross section (coherent and incoherent) from the measurement of total attenuation coefficient. The data of Jones [41] for Pb and Sn are generally higher than the calculated curves. The data of Cuykendall [42] for Al agree with the calculated curve within the experimental error. Experimental data in the region of the Hulme calculations are within the error estimated for the calculations (4% in Pb; about 8% in Sn). Although

[15] The data for Pb, I, and Cu is from L. Katz et al. for the natural elements (private communication with E. G. Fuller). The data for C is from L. Katz and A. G. W. Cameron, Can. J. Phys. **29**, 518 (1951).

[16] For tabulations of the oscillator strength for photoeffect on the K, L, and M shells as calculated from Stobbe formulas, see Lewis [40].

[17] Notice that the ratios in table 5 are substantially lower than the standard ratio 5/4, which is often utilized in the literature (see the discussion on p. 5). This difference is reflected in the difference between the photo effect cross sections given in this Circular and in the tables by Davisson and Evans [3].

measurements of total cross section at energies of 0.411, 0.511, and 0.655 Mev were made with high accuracy, an error of a few percent may result in the photoeffect cross section due to uncertainty in the cross section used for coherent scattering (see section 3.2). A direct measurement of the photoeffect cross section for 0.511 Mev γ-rays on the K shell of Pb by Seeman [43] gives a value 7 percent above the Hulme calculation. The result is within the combined error of the calculation and the experiment (3%). Additional direct measurements of the photoeffect cross section in this energy region would be very desirable.

Discussion of data for $h\nu<0.1$ Mev. The data in this energy range are fairly numerous for low-Z materials but only moderately accurate ($\sim$10%). Exceptions are the data from Cuykendall, Hubbell,[18] and French,[19] with errors of 2 to 5 percent. Data used for this comparison were assembled from Allen [44], Grosskurth [45], Cuykendall and Hubbell, as well as empirical data from Victoreen [46] and a British group.[20] Even though there is considerable variation among the data and obvious errors in spots, there is a general trend toward values for the experimental data higher than calculated from the Sauter-Stobbe formula. Empirical correction factors were obtained by this comparison and are given in table 4; the data presented in the main table are obtained by applying these corrections to the Sauter-Stobbe calculations. A theoretical interpretation of these corrections is indicated in footnote 7. The measurements by French (which were not available for the above comparison) suggest that for Al no corrections might actually have been required.

The estimated uncertainty in the calculated cross sections tabulated in this report for the photoelectric effect varies from 5 to 15 percent. Great improvement could be made in the low-energy region by a systematic study (either theoretical or experimental) especially for low-Z elements.

3.2. Scattering by Atomic Electrons

Column 2 of tables 12 to 40 gives the cross sections for coherent and incoherent scattering by the electrons of various atoms. These data represent total scattering cross sections because scattering by particles other than atomic electrons contributes to the total scattering cross section an amount smaller than the estimated error of the data. The binding of the electrons within the atoms was taken into account by methods discussed in section 2.2. To obtain the total cross section, the numerical values of the separate differential cross sections (10) and (11) were calculated numerically for a number of values of the scattering angle θ, then added, and finally integrated numerically over all directions of scattering. The contribution of either the coherent or the incoherent process was neglected at any θ where it amounts to less than 0.5 percent of the other. Thereby each of the cross sections was omitted just in the range of variables where its accuracy is lowest, that is, incoherent scattering was omitted where the momentum transfer to the atomic electrons is small (low photon energy, small scattering angle) and coherent scattering where the momentum transfer is large.

The incoherent scattering function $S(q,Z)$ that was entered in (10) is derived from the Thomas-Fermi theory of atomic structure. The numerical values utilized are given in the second column of table 41 and are discussed in the appendix. The form factor $F(q,Z)$ to be entered in (11) consists of an integral over the density distribution of atomic electrons [22]. The density distribution given by the Thomas-Fermi model was utilized at $Z>26$ for all values of q, and at $Z\leq 26$ only for large values of q. For $Z\leq 26$ and for small q, the values of $F(q,Z)$ tabulated by James and Brindley [47] and by Compton and Allison [48] served as a basis. These values utilize electron distributions derived from Hartree wave functions. Further corrections were made on the values of $F(q,Z)$ for C, N, O, utilizing more recent data of [22].[21]

For the high-Z elements, where photoelectric absorption edges occur the cross section for coherent scattering departs substantially from the form (11) as indicated in section 2.2. and is no longer a smooth function of energy. Hönl [49] [22] investigated the variation of the coherent scattering cross section in regions of anomalous dispersion and calculated particularly its decrease in the region of the K absorption edge. A rough calculation indicates an error of 10 to 20 percent in the cross section for elements from U to Mo, giving an error of less than 3 percent in the total cross section at an energy just below that of the K edge.

Experimental measurements of the cross section for coherent scattering consist mainly of data for very small or very large [51] momentum changes q of the photon. The data for small q have been reviewed [22]. The only measurements of direct interest for comparison with the calculations of this Circular were made by Storruste [52] and Mann [53]. At 0.411 Mev both sets of data show good agreement with the Thomas-Fermi form factor calculations for Pb. At photon energies of 0.662 Mev for Sn and Pb and of 1.33 for Pb, Mann's data still show satisfactory agreement at angles of scattering in the range of the calculations of the present paper.

[18] J. Hubbell (private communication).
[19] R. L. French (private communication, measurements for Al and Cu.).
[20] The data are from Hospital Physicists Association, C. 3. 1. 3. 1 and A. 3. 1. 2. (1–4) % Mr. F. S. Stewart, Mount Vernon Hospital, Northwood, Middlesex, England.

[21] A survey was made to estimate the sensitivity of the total cross sections to further improvements in the values of $F(q,Z)$, which could be introduced on the basis of [22]. These improvements would modify the total scattering cross sections by no more than 5 percent and the total absorption coefficient by no more than 1 percent.
[22] See Compton and Allison [48, p. 315] and also Parratt and Hempstead [50].

Tabulation excluding coherent scattering. Coherent scattering has usually a minor influence on the penetration of X-rays under conditions other than "narrow beam", because it is accompanied by no energy loss and by a deflection that is most frequently negligible. Therefore, this process has been disregarded in many studies, and it becomes desirable to provide data on absorption coefficients that do not include any contribution from coherent scattering. Column 3 of tables 12 to 40 gives a scattering cross section that is simply the Klein-Nishina cross section of one electron, as given in table 2, multiplied by the number of electrons Z.

3.3. Pair Production

The Bethe-Heitler Born approximation calculation was used as a zero approximation to the pair production cross section in the field of the nucleus for all Z's.

For $h\nu \leq 10\ mc^2$, screening effects are negligible and the cross section for an unscreened nucleus was obtained from the formula of Hough [54], which fits numerically the Bethe-Heitler results to within 0.1 percent. For $h\nu > 10\ mc^2$, the Bethe-Heitler formula given in [2, p. 260] was utilized and was integrated numerically over the energy distribution between the pair particles. Interpolation in Z is easily accomplished as the cross section in units of $r_0^2Z^2/137$ is a smooth and slowly varying function of Z, particularly in the low-energy region. For $h\nu > 30$ Mev the interpolation is further helped by plotting $F = \sigma_{\text{Pair}}/(r_0^2Z^2/137) + (28/27)\ln Z$ against $\gamma = 100mc^2/h\nu Z^{1/3}$.[23] Table 6 indicates the dependability of this procedure by showing that the relationships between F and γ for Al and Pb are almost identical for $h\nu > 15$ Mev.

Corrections to the Born approximation values were applied at all energies. These corrections depend primarily upon the theoretical calculations of Jaeger and Hulme [28, 29] at low photon energy ($h\nu < 10\ mc^2$) and of Davies, Bethe, and Maximon [30] at high photon energy ($h\nu >> 10\ mc^2$).

The calculations of Jaeger and Hulme have been verified in several experiments including those of Dayton [55], Hahn et al. [56], and Schmid and Huber [57]. These authors measured relative pair production cross sections at $h\nu \leq 2.62$ Mev and fitted their data by Z-dependent formulas of the form $\sigma_{\text{Pair}} = \sigma_{\text{Born}}(1 + aZ^2)$, assuming that the Born approximation is correct in the limit of low Z. Schmid [58] measured the absolute pair cross section for Pb with Co^{60} and Na^{24}. These calculations served as a basis for graphical interpolation, as illustrated by the plot of the ratios $\sigma_{\text{Pair}}/\sigma_{\text{Born}}$ for Pb on the left side of figure 4.

Following the work of Davies, Bethe, and Maximon [30] see section 2.3) a correction to the Born approximation for $h\nu > 5$ Mev was obtained by fitting a semiempirical formula

$$\sigma_{\text{Pair}} = \sigma_{\text{Born}} - \Delta\sigma_c + a^2 \frac{\ln \epsilon}{\epsilon}, \qquad (14)$$

where ϵ is the photon energy in mc^2, σ_{Born} is the Bethe-Heitler cross section for a screened nucleus, $\Delta\sigma_c$ is the Coulomb correction calculated in reference [30] for the high-energy limit, and a^2 is a constant to be determined from experimental data. Values of $\Delta\sigma_c$ and a^2 for a few Z are given in table 7. The values of a^2 were determined primarily from the data of Paul [59] and Colgate [5] at 6.13 Mev, except at low Z.

In the fitting of a^2 much weight was given to the requirement that the plot of (13) extrapolate smoothly to the experimental data and to the Jaeger-Hulme calculation results at low energy ($h\nu \lesssim 2.6$ Mev). This requirement caused the final estimates of σ_{Pair} to fall 4 to 5 percent below the estimates drawn from experimental data for Al and C at higher energies ($h\nu > 6$ Mev). This descrepancy does not appear serious because the main experimental evidence is derived from measurements of total attenuation coefficients from which one must subtract the contributions of other processes. For low-Z elements the contribution from triplet formation is considerable. This contribution has to be estimated theoretically and deducted from the measured absorption coefficient to obtain the experimental values of σ_{Pair}. The use of Vortruba's calculation rather than those of Borsellino or Wheeler and Lamb makes up to 8 percent difference in the estimate of σ_{Pair} in C, but much less (1 to 2%) for Al around 17 to 20 Mev. The contribution from photonuclear processes is likewise relatively more important for low-Z elements. Differences of about 5 percent in the estimate of σ_{Pair} for $Z \leq 29$ are caused by assuming an uncertainty of 100 percent in the cross section for the production of neutrons. The values of σ_{Nuclear} used to reduce the data entered in figure 4 were taken from various sources of experimental data on the photonuclear processes. For $Z \leq 13$ it was assumed that the probability for production of protons equals the probability for production of neutrons.

The data at 6.13 Mev were given much weight in fitting a^2 for $Z \geq 29$ to minimize the uncertainties in unraveling the pair production cross section from total attenuation coefficients. This energy lies below the threshold of the main photonuclear processes. With regard to the photoelectric effect, at 6.13 Mev its contribution to the total absorption is small even in Pb. On the other hand, fitting a^2 at large energies, above the range of large photonuclear cross sections, would yield low accuracy because the value of $\epsilon^{-1} \ln \epsilon$ becomes quite small.

A complete curve of the ratio $\sigma_{\text{Pair}}/\sigma_{\text{Born}}$ is given in figure 4 for Pb, with all the relevant

[23] A theoretical interpretation of this procedure is given in [2].

experimental data. The curves thus obtained by fitting a^2 in (4) agree with all experimental data satisfactorily except for the data of Rosenblum et al. [60] at 5.13 and 10.3 Mev, where they are well outside the experimental error stated by the authors.

The curve for iodine in figure 5 shows a comparison of calculated ratios of $\sigma_{Pair}/\sigma_{Born}$ by West [61], using experimental data derived from various sources including his own measurement of absolute and relative pair production cross sections in sodium iodide using sources of Co^{60} and Na^{24}. This comparison is especially interesting since most of the data for iodine was calculated using Z-dependence formulas determined by the various authors. Agreement is mostly within the experimental errors, excluding the data of Rosenblum et al. at 5.13 and 10.3 Mev. The data of West at 1.17 Mev are the only ones available at this low energy and cannot be compared directly with other experimental or theoretical data. They indicate an increase in the ratio $\sigma_{Pair}/\sigma_{Born}$ as the threshold energy is approached more rapidly than expected by the extrapolation carried out in the figure.

Generally, experimental data fit the calculated curves within experimental errors of a few percent. The estimated error in the pair cross sections given in the main table is about 3 percent except at the lowest energies (<3 Mev) and in the region where absorption by the nuclear photoeffect is important (10 to 30 Mev).

Pair Production in the electron field. Calculations of the pair cross section in the field of electrons were made by using the formula of Vortruba (12) and (13). Graphical interpolation was made in the energy region where the two formulas were not valid. This was accomplished by assuming the validity of the formulas to be less restricted than indicated and also by using the calculations of Borsellino [31] (see 2.3) as a guide to the shape of a curve of $\sigma_{Electron}/\sigma_{Proton}$.

It is difficult to assign an error to this estimate. There are no direct measurements of the cross section for pair production with electron recoil (triplet production). Some evidence is obtained indirectly from measurements of the total absorption coefficient in hydrocarbons [62] and also from measurements on the related process of bremstrahlung [34] (see footnote 13). However the weight of this evidence is diluted in the process of extracting information on the triplet process, and the resulting accuracy is not adequate to improve the theoretical estimates.

3.4. Total Attenuation Coefficient

Total cross sections were obtained by summing the cross sections for the individual absorption and scattering processes discussed (3.1, 3.2, and 3.3). Cross sections for nuclear processes are *not* included for the reasons indicated in 2.4. The results are given in tables 12 to 40. Cross sections for the individual processes are expressed in barns (10^{-24} cm^2), and the total absorption coefficient is given as a mass coefficient in square centimeters per gram. Conversion factors from barns to square centimeters per gram are tabulated for each Z. Attenuation coefficients with and without the contribution of coherent scattering (see section 3.2) are given separately. The purpose for which the data are used will determine the choice between the two sets of data.

In general, data are tabulated with a number of digits such that the uncertainty in the last digit amounts to a very few units. However, the total attenuation data are given throughout with three digits, for purpose of smoothness, even when the last digit may be in substantial error.

The estimated errors have been discussed in some detail in the preceding sections. A comparison of the tabulated total absorption coefficients with experimental data is shown in tables 8 to 11. As an over-all estimate, the errors may easily approach 10 percent below 50 kev, especially for light elements, but probably do not exceed 3 to 5 percent above 100 kev.

The author thanks the large number of persons who assisted in the preparation of this Circular by contributing generously of their time and information in discussions and by correspondence. The cooperation of U. Fano in the preparation of the manuscript is greatly appreciated.

4. Figures and Tables

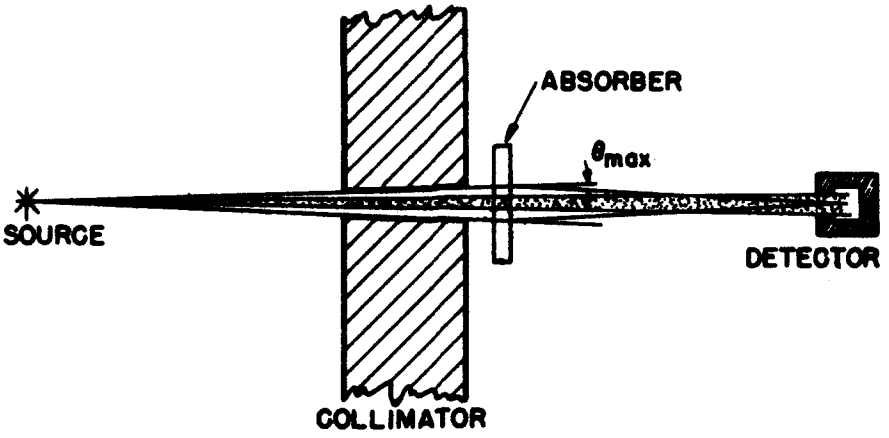

FIGURE 1. *Experimental arrangement in measuring "narrow-beam" attenuation coefficients.*

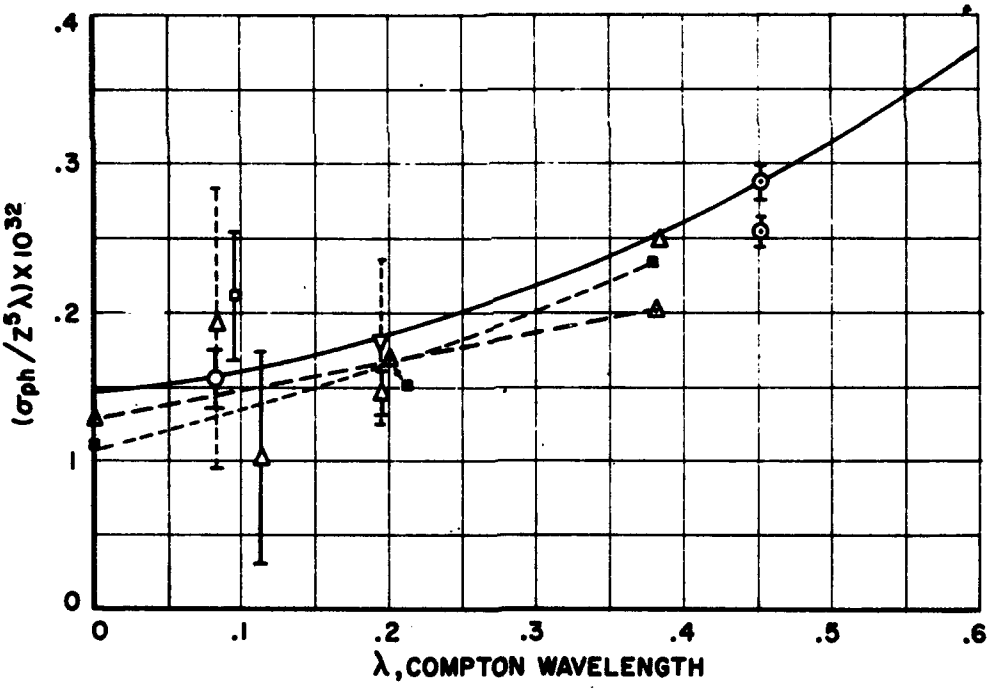

FIGURE 2. *Data analysis and interpolation for the photoelectric cross section of Pb at energies* >1 *Mev.*

Calculated data:

⊙, Hulme [15].
△, Hall [16, 10].
⊡, Nagasaka [17]. } *K* shell only.

Experimental data:

▽, Latyshev [18] direct observation.
△, Colgate [5].
○, Paul [59]. } Total absorption coefficient less an estimate of other absorption and scattering processes.
□, Rosenblum [60].

——, values used.

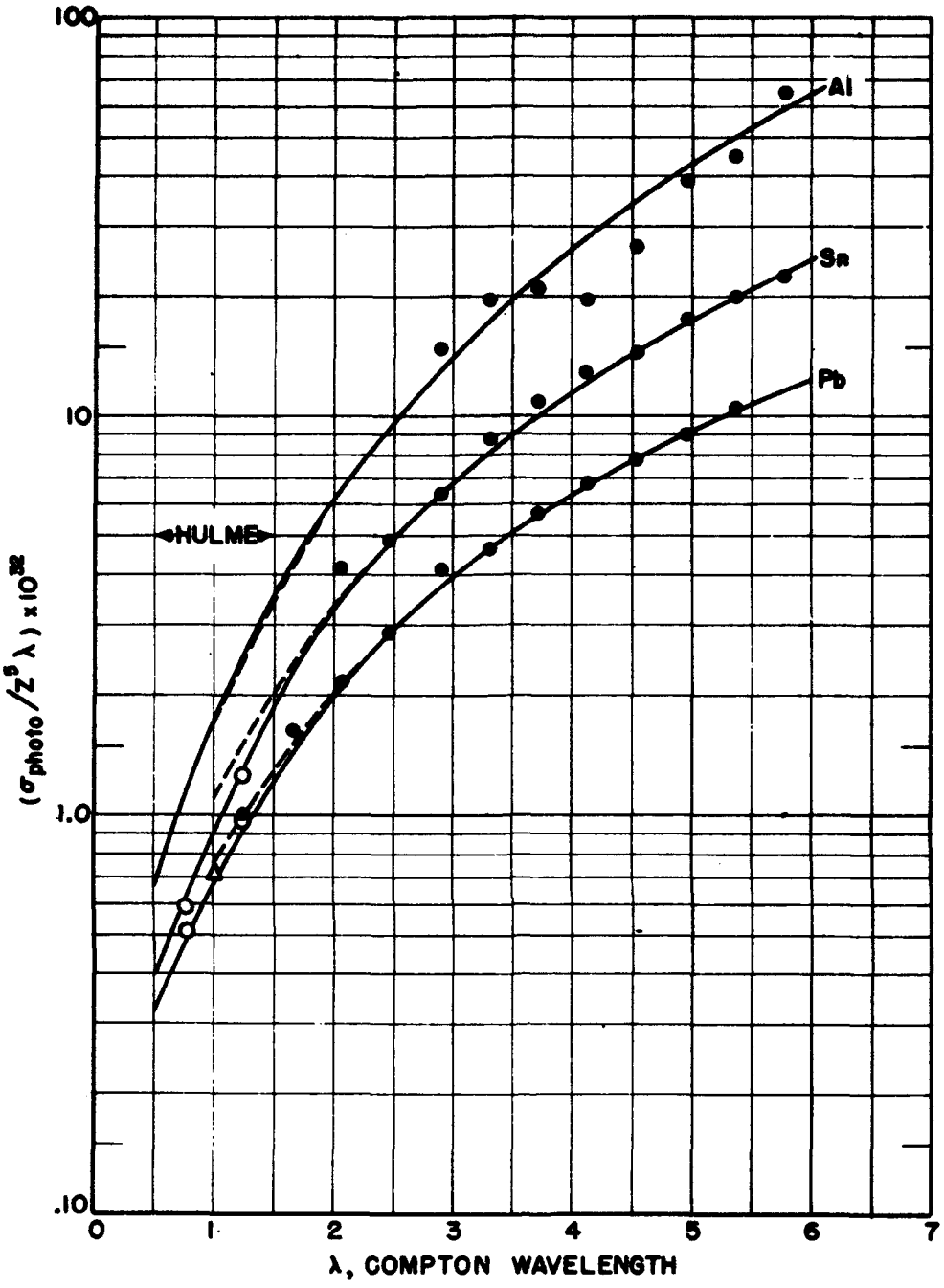

FIGURE 3. *Data analysis and interpolation for the photoelectric cross section for lead, tin, and aluminum from 0.1 to 1 Mev.*

The solid curves are drawn through the Sauter-Stobbe points at large values of λ and through the Hulme calculations (adjusted by the contribution of the L and M shells) in the indicated region. Values used in the present circular were taken from the solid curves. The dashed curves show the departure of the Sauter-Stobbe from the Hulme values. Experimental data were obtained by subtracting scattering (coherent+incoherent) from the measured total attenuation coefficients.

●, Jones-Cuykendall [41, 42]; ○, Colgate [5]; △, Seeman [43]

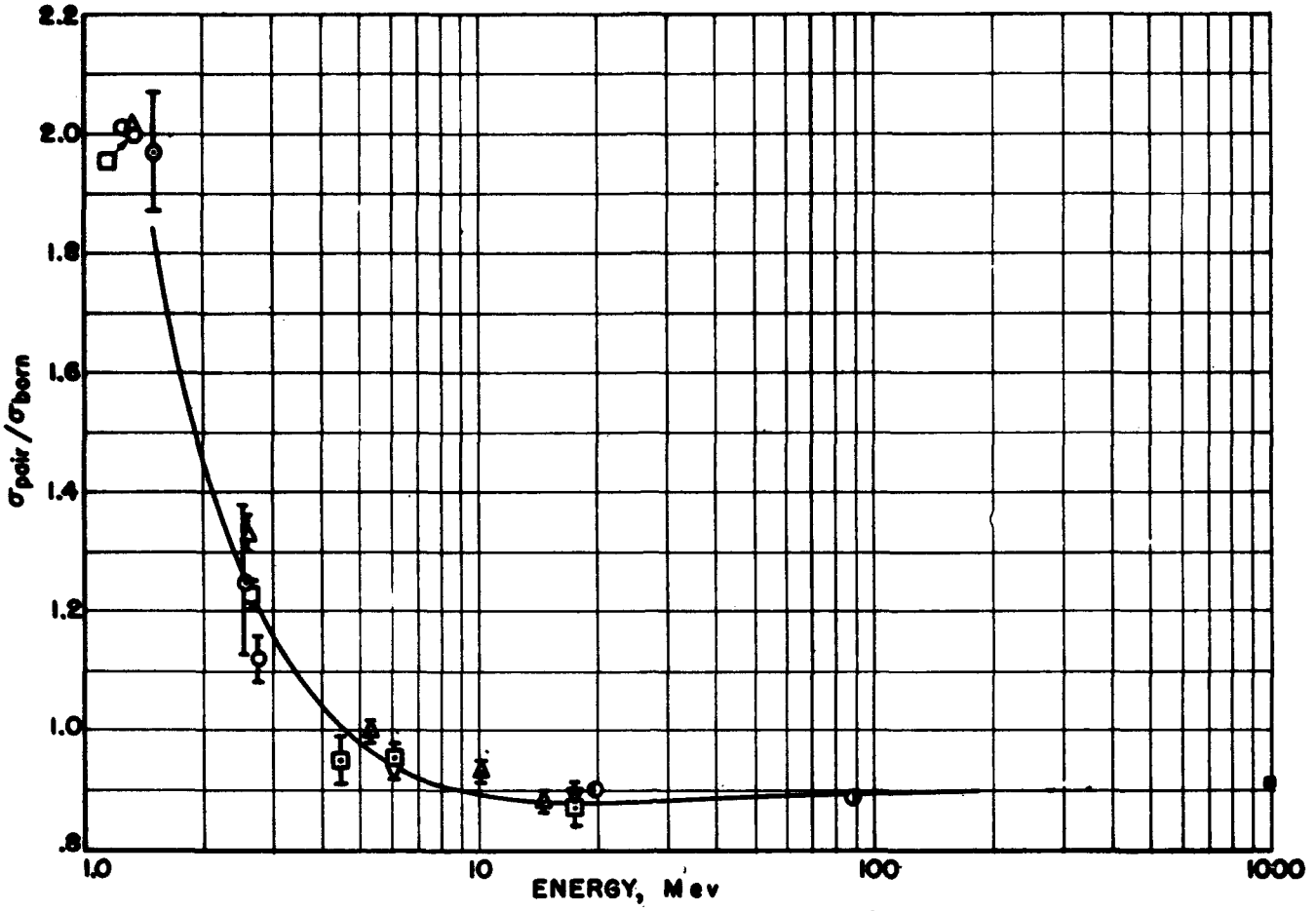

FIGURE 4. *The ratio $\sigma_{Pair}/\sigma_{Born}$ for lead.*

Calculated data: ⊙, Kaeger [28, 29]; ■ Davies et al. [30].
Experimental data:

○, Schmid [57, 58].
□, Dayton [55].
△, Hahn et al. [56].
⊡, Colgate [54].
▲, Rosenblum [60].
▽, Paul [59].
▽, Walker [53].
◐, Berman [65].
◑, Lawson [66].
●, Dewire [67].

———, values used.

The significance of the experimental data plotted in this figure is discussed in section 3.3.

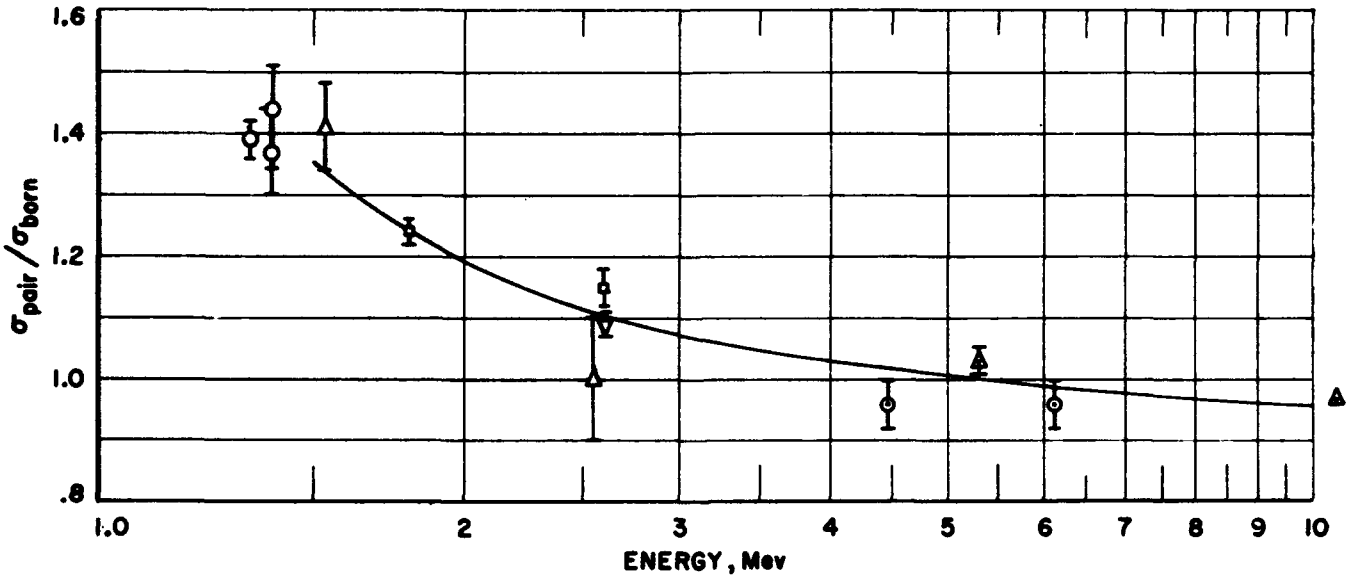

FIGURE 5. *The ratio $\sigma_{Pair}/\sigma_{Born}$ for iodine.*

Calculated data: △, Jaeger [29]; □, Hahn et al. [56].
Experimental data: ○, West [61]; ▽, Dayton [55]; ⊙, Colgate [5]; ▲, Rosenblum [60].
———, values used

The significance of the experimental data plotted in this figure is discussed in section 3.3.

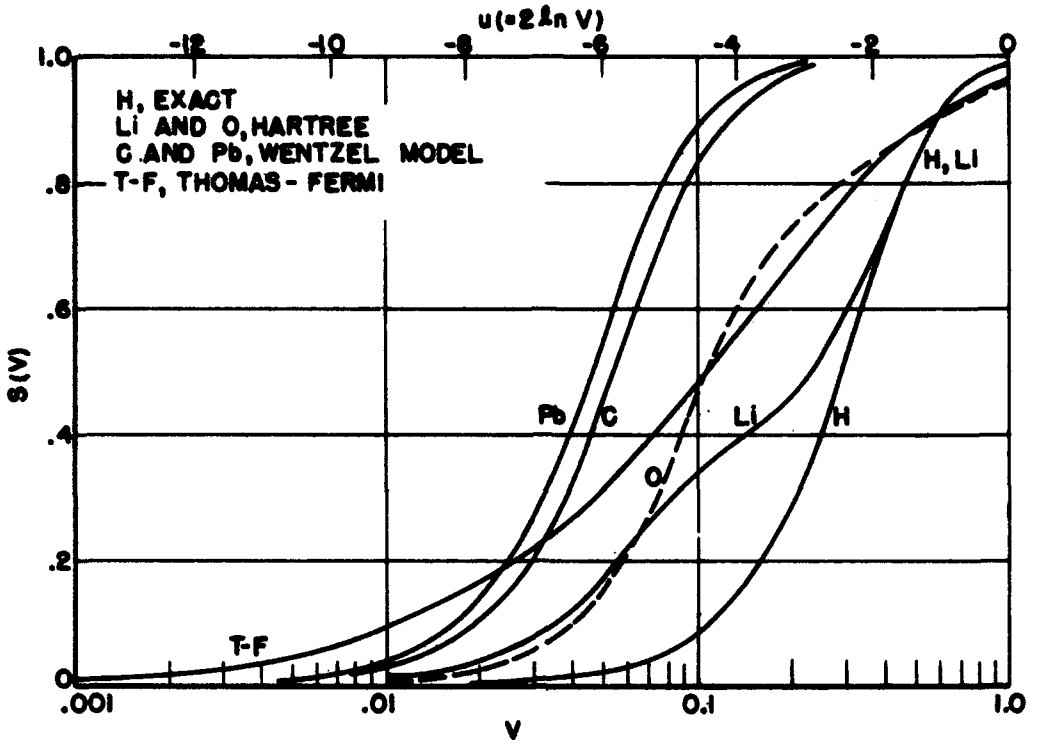

FIGURE 6. *Incoherent scattering function S(v), for* H, Li, C, O, *and Pb.*

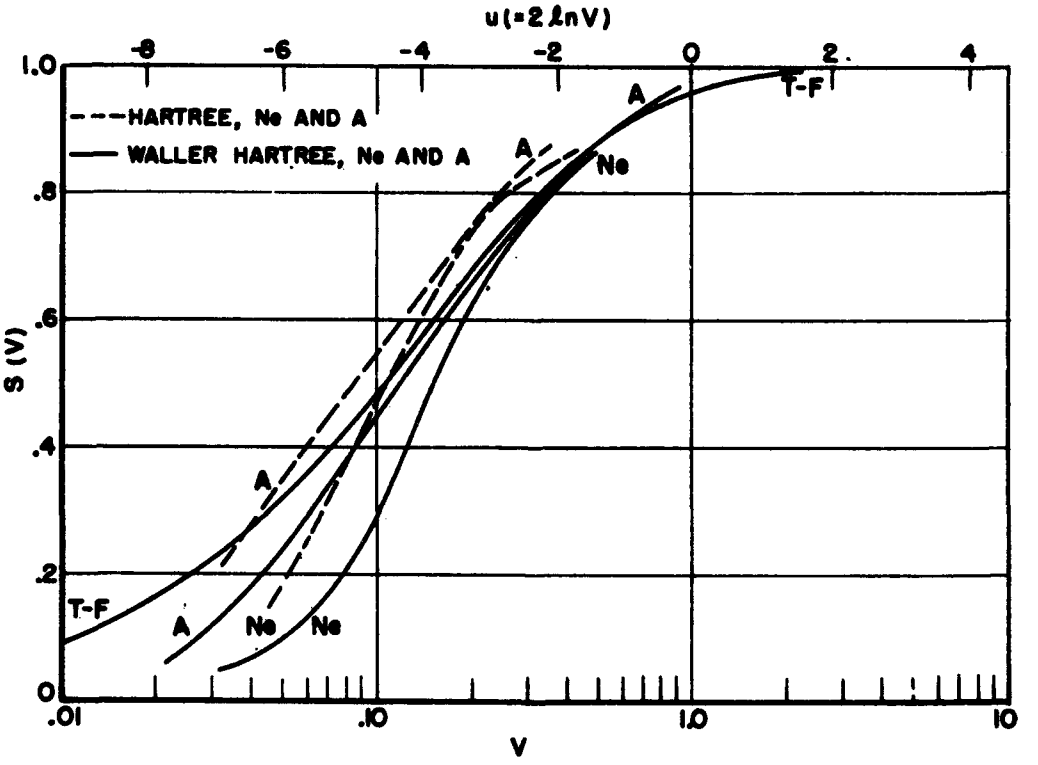

FIGURE 7. *Incoherent scattering function S(v) for* Ne *and* A.

TABLE 1. *Slater screening constant for different electron groups*

Atomic number	Electron groups				
	1s	2s or 2p	3s or 3p	3d	4s or 4p
2	0.30				
3	↓	1.70			
4	↓	2.05			
5	↓	2.40			
6	↓	2.75			
7	↓	3.10			
8	↓	3.45			
9	↓	3.80			
10	↓	4.15			
11	↓	↓	8.80		
12	↓	↓	9.15		
13	↓	↓	9.50		
14	↓	↓	9.85		
15	↓	↓	10.20		
16	↓	↓	10.55		
17	0.30 for all Z	↓	10.90		
18	↑	↓	11.25		
19	↑	↓	↓		16.80
20	↑	↓	↓		17.15
21	↑	↓	↓	18.00	18.00
22	↑	4.15 for all Z	↓	18.35	18.35
23	↑	↑	↓	18.70	19.70
24	↑	↑	↓	19.40	21.05
25	↑	↑	↓	19.40	21.40
26	↑	↑	↓	19.75	22.25
27	↑	↑	↓	20.10	23.10
28	↑	↑	11.25 for	20.45	23.95
29	↑	↑	all Z	21.15	25.30
30	↑	↑	↑	↓	25.65
	↑	↑	↑	21.15 for	
	↑	↑	↑	all Z	
	↑	↑	↑	↑	

TABLE 2. *Cross section calculated from the Klein-Nishina formula*

Photon energy	Square centimeters per electron	Photon energy	Square centimeters per electron
Mev		*Mev*	
0.010	0.640×10^{-24}	1.0	0.2112×10^{-24}
.015	.629	1.5	.1716
.020	.618	2.0	.1464
.030	.597	3.0	.1151
.040	.578	4.0	.0960
.050	.561	5.0	.0826
.060	.546	6.0	.0732
.080	.517	8.0	.0599
.10	.4939	10	.05100
.15	.4436	15	.03773
.20	.4066	20	.03024
.30	.3535	30	.02199
.40	.3167	40	.01746
.50	.2892	50	.01456
.60	.2675	60	.01264
.80	.2350	80	.00988
		100	.00830

TABLE 3. *Comparison of the sum of the scattering cross section, including coherent, the photoelectric, and the pair cross sections with the photoneutron cross section, in barns*

Z	Energy (Mev)														
	10	12	13.2	14	15.2	16	18	19.2	20	21	22	23	24	25	26
Pb	16.8 0.2	17.7 0.5	18.3 0.84	18.6 0.8	---- ----	19.5 0.4	20.3 0.2								
I	----	8.66 0.16	----	9.02 0.36	9.24 0.47	9.37 0.41	9.66 0.31	---- ----	9.96 0.19						
Cu	----	----	----	3.32 0.05	---- ----	3.38 0.09	3.45 0.11	3.49 0.12	3.52 0.11	---- ----	3.59 0.08				
C [1]	----	----	----	----	----	----	----	----	----	0.303 .002	0.300 .009	0.297 .013	0.294 .009	0.292 .005	0.289 .003

[1] A cross section of the same order of magnitude is expected for proton emission as for neutron emission.

TABLE 4. *Correction factors applied to the Sauter-Stobbe formula at photon energy of .10 to 100 kev*

Photon energy	Element														
	Be	C	N	O	Na	Mg	Al	Si	P	S	A	K	Ca	Fe	Cu
kev															
10	1.14	1.13	1.13	1.12	1.11	1.11	1.10	1.10	1.10	1.09	1.08	1.08	1.08	1.06	1.05
15	1.11	1.11	1.10	1.10	1.09	1.09	1.09	1.08	1.08	1.08	1.07	1.07	1.07	1.05	1.04
20	1.09	1.09	1.08	1.08	1.08	1.08	1.08	1.07	1.07	1.07	1.06	1.06	1.06	1.04	1.04
30	1.06	1.06	1.06	1.06	1.06	1.06	1.06	1.06	1.06	1.06	1.05	1.05	1.05	1.03	1.03
40	1.05	1.05	1.05	1.05	1.05	1.05	1.05	1.05	1.05	1.05	1.04	1.04	1.04	1.03	1.02
50	1.04	1.04	1.04	1.04	1.04	1.04	1.04	1.04	1.04	1.04	1.04	1.03	1.03	1.02	1.02
60	1.03	1.03	1.03	1.03	1.03	1.03	1.03	1.03	1.03	1.03	1.03	1.03	1.03	1.02	1.01
80	1.03	1.03	1.03	1.03	1.03	1.03	1.03	1.02	1.02	1.02	1.02	1.02	1.02	1.01	1.01
100	1.02	1.02	1.02	1.02	1.02	1.02	1.02	1.02	1.02	1.02	1.02	1.02	1.02	1.01	1.01

TABLE 5. *The ratio σ_{K+L+M}/σ_K calculated from the Stobbe formulas*

Z	K edge	340 kev
6	1.02	1.01
8	1.03	1.02
13	1.05	1.03
18	1.07	1.04
26	1.10	1.06
29	1.11	1.07
42	1.13	1.09
50	1.14	1.10
74	1.161	1.124
82	1.164	1.131
92	1.167	1.138

TABLE 6. *The function $F(\gamma)$ for* Al *and* Pb

γ	Al		Pb	
	$h\nu$	$F(\gamma)$	$h\nu$	$F(\gamma)$
	Mev		*Mev*	
0.1	217	13.8	118	13.8
.15	147	13.1	78.4	13.1
.2	107	12.5	58.8	12.5
.4	54.3	10.9	29.4	10.9
.6	36.2	9.82	19.6	9.82
.8	27.2	9.03	14.7	9.06
1.0	21.7	8.41	11.8	8.51
1.5	14.5	7.29	7.84	7.50
2.0	10.7	6.49	5.88	6.83
2.5	8.69	5.91	4.70	6.34

TABLE 7. *The Coulomb correction $\Delta\sigma_c$ and the energy dependent term a^2 of the empirical correction*

Z	$\Delta\sigma_c$	a^2
	Barns	*Barns*
13	0.0032	0.0159
29	.079	.380
42	.333	1.61
50	.649	3.14
53	.809	3.72
74	2.78	11.8
78	3.36	14.0
82	4.02	16.8
92	6.03	24.7

TABLE 8. *Comparison of calculated and measured total attenuation coefficient [cm²/g] for* Pb

Energy	Calculated	Victoreen [46] (empirical)	Jones [41] (~2%)	Colgate [5]	Argyle [70]	Cowan[a] [69]	Davisson [3]	Schmid and Huber [57]	Wyard [71] (0.5 to 1.0%)	Rosenblum [60]	Paul [59]	Adams [65]	Walker [63]	Berman [66]	Lawson [62]
Mev															
0.0954	6.21	----	6.412												
.103	5.06	5.010	5.150												
.113	3.92	----	4.079												
.124	3.06	3.163	3.248												
.136	2.32	----	2.490												
.155	1.75	1.780	1.839												
.177	1.26	----	1.455												
.207	0.870	0.8507	0.900												
.248	.575	.5403	.600												
.279(Hg^{203})	.440	----	----	----------	----------	----	----	----------	0.454						
.310	.354	.3210	.394												
.325(Cr^{51})	.323	----	----	----------	----------	----	----	----------	.335						
.411(Au^{198})	.209	----	----	0.2131±0.15%											
.413	.208	.1776	.22												
.496(Ru^{103})	.154	.1296	----	----------	----------	----	----	----------	.151						
.511(Annh.)	.142	----	----	----------	0.1519±0.53%	----	----	0.1421±3.9%							
.664(Cs^{137})	.106	----	----	.1072±.19%	----------	0.112									
.835(Mn^{54})	.0826	----	----	----------	----------	----	0.0830								
1.076(Rb^{86})	.0658	----	----	----------	----------	----	----	----------	.0645						
1.11 (Zn^{65})	.0640	----	----	----------	----------	.0641	.0626								
1.25 (Co^{58}, avg)	.0586	----	----	----------	----------	----	.05754	----------	.0573						
1.33 (Co^{60})	.0561	----	----	.0553±.18%											
1.51 (K^{42})	.0521	----	----	----------	----------	----	----	----------	.0505						
1.71 (Sb^{124})	.0492	----	----	----------	----------	.0472									
2.62 (ThC'')	.0430	----	----	.04206±.34%											
2.76 (Na^{24})	.0427	----	----	----------	----------	.0419	.0423								
4.47	.0423	----	----	.0413±2%											
5.3	.0429	----	----	----------	----------	----	----	----------	----	0.04282±1.0%					
6.13	.0437	----	----	.0430±2%	----------	----	----	----------	----	----------	0.04350				
10.3	.0492	----	----	----------	----------	----	----	----------	----	.05185±1.0%					
11.04	.0503	----	----	----------	----------	----	----	----------	----	----------	----	0.05013±1.2%			
13.73	.0539	----	----	----------	----------	----	----	----------	----	----------	----	.05508±1.1%			
17.6	.0586	----	----	.0590±2%	----------	----	----	----------	----	.05953±1.0%	----	----------	0.5979±0.6%		
19.10	.0602	----	----	----------	----------	----	----	----------	----	----------	----	.06134±0.6%			
19.5	.0606	----	----	----------	----------	----	----	----------	----	----------	----	----------	----------	0.06275±0.28%	
88.0	.0917	----	----	----------	----------	----	----	----------	----	----------	----	----------	----------	----------	0.09098±1.6%

[a] Linear absorption coefficients were converted into units of cm²/g by using ρ=11.29 (Davisson's value).

TABLE 9. *Comparison of calculated and measured total attenuation coefficients [cm²/g] for* Sn

Energy	Calculated	Victoreen [46] (empirical)	Jones [41] (~2%)	Cowan [a] [69]	Colgate [5]	Davisson [3]	Schmid and Huber [57]	Rosenblum [60]	Paul [58]	Walker [63]	Berman [65]	Lawson [66]
Mev												
0.0310	38.7	38.46										
.0413	17.6	18.61										
.0496	10.8	11.49										
.0620	5.90	6.324										
.0827	2.70	2.871										
.0886	2.26	----------	2.310									
.0954	1.85	----------	1.912									
.103	1.53	1.571	1.567									
.113	1.20	----------	1.222									
.124	0.960	0.9733	1.020									
.138	.740	----------	0.800									
.155	.561	.5581	.607									
.177	.420	----------	.430									
.207	.305	.2942	.314									
.248	.220	.2078	.246									
.310	.156	.1466										
.325 (Cr^{51})	.145	----------	------	0.144								
.411 (Au^{198})	.111	----------	------	------	0.1095±0.18%							
.413	.111	.1040										
.496	.0929	.0880										
.511 (Annh.)	.0910	----------	------	------	----------	--------	0.0906±2.8%					
.664 (Cs^{137})	.0742	----------	------	.0714	.0740±1.4%							
.835 (Mn^{54})	.0642	----------	------	------	----------	0.0642						
1.11 (Zn^{65})	.0542	----------	------	.0510	----------	.0538						
1.25 (Co^{60} avg)	.0507	----------	------	------	----------	.05051						
1.33 (Co^{60})	.0490	----------	------	------	.0488±0.20%							
1.71 (Sb^{124})	.0436	----------	------	.0414								
2.62 (ThC'')	.0377	----------	------	------	.03745±0.27%							
2.76 (Na^{24})	.0373	----------	------	.0365	----------	.0366						
4.47	.0355											
5.3	.0356	----------	------	------	----------	--------	----------	0.0356±1.4%				
6.13	.0356	----------	------	------	.0346±2.3%	--------	----------	----------	0.03508			
10.3	.0366	----------	------	------	----------	--------	----------	.0404±0.99%				
17.6	.0442	----------	------	------	.0457±3%	--------	----------	.04681±1.0%	--------	0.0455±1%		
19.5	.0454	----------	------	------	----------	--------	----------	----------	--------	----------	0.0469±0.54%	
88.0	.0661	----------	------	------	----------	--------	----------	----------	--------	----------	----------	0.06655±0.95%

[a] Linear absorption coefficients were converted into units of cm²/g by using $\rho = 7.297$ (Davisson's value).

TABLE 10. *Comparison of calculated and measured total attenuation coefficients [cm²/g] for* Cu

Energy	Calculated	Victoreen [46] (empirical)	Guy-Kendall [42] (~2%)	Cowan[a] [69]	Colgate [5]	Argyle [70]	Davisson [3]	Wyard [71] (0.5 to 1%)	Schmid and Huber [57]	Howland and Kreger [72]	Rosenblum [60]	Paul [50]	Adams [62]	Walker [63]	Berman [65]	Lawson [66]
Mev.																
0.0103	206	201.4														
.0155	70.5	70.38														
.0207	31.7	32.02														
.0248	19.2	19.25														
.0310	10.1	10.26														
.0413	4.44	4.561														
.0496	2.64	2.741														
.0568	1.62	----	1.63													
.0620	1.45	1.495														
.0674	1.16	----	1.17													
.0775	0.827	----	0.830													
.0827	.710	0.7180														
.0886	.606	----	.606													
.0954	.513	----	.513													
.103	.432	.4323	.434													
.113	.356	----	.371													
.124	.301	.3018	.306													
.136	.261	----	.259													
.155	.213	.2102	.215													
.177	.179	----	.183													
.207	.150	.1486	.160													
.248	.129	.1256	.129													
.279(Hg [203])	.117	----	----	----	----------	---------	---	0.116								
.310	.110	.1073														
.325(Cr [51])	.106	----	----	0.1050	----------	---------	---	.105								
.411(Au [198])	.0926	----	----	----	0.0912±0.16%											
.413	.0921	.0907														
.496	.0836	.0826	----	----	----------	---------	---	.0816								
.511(Annh.)	.0826	----	----	----	----------	0.819±0.61%	---	----	0.0820±5.4%							
.664(Cs [137])	.0720	----	----	.0691	.0721±0.14%	---------	---	----	---------	0.0727±0.29%						
.835(Mn [54])	.0642	----	----	----	----------	---------	0.0648									
1.076(Rb [86])	.0566	----	----	----	----------	---------	---	.0567								
1.11 (Zn [65])	.0556	----	----	.0535	----------	---------	.0545	----	---------	.0557±0.54%						
1.25 (Co [60], avg)	.0522	----	----	----	----------	---------	.05257	.0521								
1.33 (Co [60])	.0505	----	----	----	.05062±0.3%											
1.51 (K [42])	.0473	----	----	----	----------	---------	---	.0472								
1.71 (Sb [124])	.0446	----	----	.0416												
2.62 (ThC″)	.0375	----	----	----	.0375±0.27%											
2.76 (Na [24])	.0368	----	----	----	----------	---------	.0354									
4.47	.0322															
5.3	.0314	----	----	----	----------	---------	---	----	----------	----------	0.03076±0.99%					
6.13	.0309	----	----	----	.0300±2.3%	---------	---	----	---------	---------	----------	0.03086				
10.3	.0306	----	----	----	----------	---------	---	----	---------	---------	.03115±0.91%					
11.04	.0308	----	----	----	----------	---------	---	----	---------	---------	----------	---	0.0309±1.1%			
13.73	.0315	----	----	----	----------	---------	---	----	---------	---------	----------	---	.0319±1.1%			
17.6	.0328	----	----	----	.0330±2%	---------	---	----	---------	---------	.03497±1.1%	---	---------	0.0343±0.6%		
19.10	.0331	----	----	----	----------	---------	---	----	---------	---------	----------	---	.0343±3%			
19.5	.0332	----	----	----	----------	---------	---	----	---------	---------	----------	---	---------	---------	0.03523±0.51%	
88.0	.0449	----	----	----	----------	---------	---	----	---------	---------	----------	---	---------	---------	----------	0.0471±1.5%

[a] Linear absorption coefficients were converted into units of cm²/g by using ρ=8.927 (Davisson's value).

TABLE 11. *Comparison of calculated and measured total attenuation coefficients* [cm^2/g] *for* Al

Energy	Calculated	Victoreen [46] (empirical)	Cuykendall [42] (~4%)	Cowan [69]	Colgate [5]	Argyle [70]	Davisson [8]	Wyard [71] (0.5 to 1.0%)	Schmid and Huber [57]	Paul [59]	Adams [68]	Walker [63]	Berman [65]	Lawson [66]
Mev														
0.0103	24.5	23.68												
.0155	7.30	7.318												
.0207	3.15	3.226												
.0248	1.92	1.950												
.0310	1.04	1.067												
.0413	0.524	0.5573												
.0496	.368	.3882												
.0568	.275	------	0.279											
.0620	.259	.2740												
.0674	.234	------	.240											
.0775	.203	------	.213											
.0827	.193	.1985												
.0886	.183	------	.191											
.0954	.174	------	.176											
.103	.166	.1672	.168											
.113	.157	------	.158											
.124	.151	.1502	.150											
.138	.143	------	.144											
.155	.136	.1353	.138											
.177	.128	------	.131											
.207	.121	.1201	.121											
.248	.113	.1112	.113											
.270(Hg^{203})	.107	------	------	------	----------	----------	------	0.106						
.310	.103	.1024												
.325(Cr^{51})	.101	------	------	0.107	----------	----------	------	.101						
.411(Au^{198})	.0918	------	------	------	0.0915±0.22%									
.413	.0916	.0910												
.496(Ru^{103})	.0846	.0845	------	------	----------	----------	------	.0842						
.511(Annh.)	.0838	------	------	------	----------	0.0831±1.6%	------	------	0.0823±5.5%					
.664(Cs^{137})	.0744	------	------	.0718	.0742±0.13%									
.835(Mn^{54})	.0668	------	------	------	----------	----------	0.0671							
1.076(Rb^{86})	.0602	------	------	------	----------	----------	------	.0591						
1.11 (Zn^{65})	.0583	------	------	.0570	----------	----------	.0578							
1.25 (Co^{60},avg)	.0550	------	------	------	----------	----------	.05527	.0547						
1.33 (Co^{60})	.0532	------	------	------	.0532±0.19%									
1.51 (K^{42})	.0499	------	------	------	----------	----------	------	.0498						
2.62 (ThC'')	.0378	------	------	------	.0378±0.26%									
2.76 (Na^{24})	.0368	------	------	------	----------	----------	.0352							
4.47	.0295													
6.13	.0263	------	------	------	.0259±1.9%	----------	------	------	----------	0.02644				
11.04	.0225	------	------	------	----------	----------	------	------	----------	------	0.02242±2.1%			
13.73	.0217	------	------	------	----------	----------	------	------	----------	------	.0221 ±1.0%			
17.6	.0212	------	------	------	.0216±2%	----------	------	------	----------	------	----------	0.0217±1.1%		
19.1	.0212	------	------	------	----------	----------	------	------	----------	------	.02237±2.6%			
19.5	.0212	------	------	------	----------	----------	------	------	----------	------	----------	----------	0.02246	
88.0	.0243	------	------	------	----------	----------	------	------	----------	------	----------	----------	------	0.02519±1.5%

[a] Linear absorption coefficients were converted into units of cm^2/g by using $\rho = 2.717$ (Davisson's value).

TABLE 12. Hydrogen

Photon energy	Scattering[a] without coherent	Photoelectric 1s electron	Pair production		Total[b] without coherent
			Nucleus	Electron	
Mev	Barns/atom	Barns/atom	Barns/atom	Barns/atom	cm^2/g
0.01	0.640	0.0046			0.385
.015	.629	.0011			.377
.02	.618				.369
.03	.597				.357
.04	.578				.345
.05	.561				.335
.06	.546				.326
.08	.517				.309
.10	.493				.295
.15	.444				.265
.20	.407				.243
.30	.354				.212
.40	.317				.189
.50	.289				.173
.60	.268				.160
.80	.235				.140
1.0	.211				.126
1.5	.1716		0.000044		.103
2.0	.1464		.00018		.0876
3.0	.1151		.00051	0.00001	.0691
4.0	.0960		.00082	.00005	.0579
5.0	.0828		.0011	.0001	.0502
6.0	.0732		.0013	.0002	.0446
8.0	.0599		.0018	.0004	.0371
10	.0510		.0021	.0006	.0321
15	.0377		.0028	.0011	.0249
20	.0302		.0033	.0015	.0209
30	.0220		.0040	.0021	.0168
40	.01746		.0045	.0026	.0147
50	.01456		.0048	.0029	.0133
60	.01254		.0051	.0033	.0125
80	.00988		.0056	.0038	.0115
100	.00820		.0059	.0042	.0109

a Total scattering for Hydrogen is given by the Klein-Nishina formula for free electrons.

b Barns/atom x 0.5997 = cm^2/g

TABLE 13. Beryllium

Photon energy	Scattering[a]		Photoelectric K and L shells	Pair production		Total[b]	
	With coherent	Without coherent		Nucleus	Electron	With coherent	Without coherent
Mev	Barns/atom	Barns/atom	Barns/atom	Barns/atom	Barns/atom	cm^2/g	cm^2/g
0.01	3.54	2.56	5.42			0.599	0.533
.015	3.01	2.52	1.39			.294	.261
.02	2.77	2.47	0.52			.220	.200
.03	2.53	2.39	.13			.178	.168
.04	2.38	2.31	.052			.163	.158
.05	2.29	2.24	.021			.154	.151
.06	2.21	2.18	.010			.148	.146
.08	2.10	2.07				.140	.138
.10	1.99	1.972				.133	.132
.15	1.78	1.774				.119	.119
.20	1.63	1.626				.109	.109
.30		1.414					.0945
.40		1.267					.0847
.50		1.157					.0773
.60		1.070					.0715
.80		0.940					.0628
1.0		.845					.0565
1.5		.686		0.00071			.0459
2.0		.586		.0028			.0394
3.0		.460		.0081	0.00005		.0313
4.0		.384		.013	.0002		.0266
5.0		.331		.018	.0004		.0234
6.0		.293		.022	.0008		.0211
8.0		.240		.028	.002		.0180
10		.204		.034	.003		.0161
15		.1509		.044	.004		.0133
20		.1210		.052	.006		.0120 *
30		.0880		.063	.008		.0106
40		.0698		.070	.010		.0100
50		.0582		.076	.012		.00977
60		.0502		.081	.013		.00964
80		.0395		.087	.015		.00946
100		.0328		.093	.017		.00955

a Data in the first column is given by the sum of coherent scattering and of incoherent scattering from the Klein-Nishina formula corrected for binding effects. In the second column incoherent scattering is given by the Klein-Nishina formula for free electrons.

b Barns/atom x 0.06684 = cm^2/g

* Energy region in which dipole absorption attains a maximum cross section.

TABLE 14. Carbon

Photon energy	Scattering[a]		Photoelectric K and L shells	Pair production		Total[b]	
	With coherent	Without coherent		Nucleus	Electron	With coherent	Without coherent
Mev	Barns/atom	Barns/atom	Barns/atom	Barns/atom	Barns/atom	cm^2/g	cm^2/g
0.01	6.88	3.84	38.6			2.28	2.13
.015	5.30	3.77	10.2			0.777	0.701
.02	4.64	3.71	3.91			.429	.382
.03	4.04	3.58	0.99			.252	.229
.04	3.71	3.47	.38			.205	.193
.05	3.50	3.37	.18			.185	.178
.06	3.37	3.28	.096			.174	.169
.08	3.18	3.10	.037			.161	.157
.10	3.02	2.96	.017			.152	.149
.15	2.69	2.66	.0040			.135	.134
.20	2.46	2.44				.123	.122
.30	2.13	2.12				.107	.106
.40		1.900					.0953
.50		1.735					.0870
.60		1.605					.0805
.80		1.410					.0707
1.0		1.267					.0636
1.5		1.030		0.0016			.0518
2.0		0.878		.0063			.0444
3.0		.691		.018	0.00007		.0356
4.0		.576		.030	.0003		.0304
5.0		.497		.040	.0007		.0270
6.0		.439		.048	.001		.0245
8.0		.359		.063	.002		.0225
10		.306		.076	.004		.0216
15		.226		.099	.006		.0166
20		.1814		.116	.009		.0154*
30		.1319		.140	.012		.0142
40		.1048		.157	.015		.0139
50		.0874		.170	.018		.0138
60		.0752		.180	.020		.0138
80		.0593		.195	.023		.0139
100		.0492		.207	.025		.0141

a Data in the first column is given by the sum of coherent scattering and of incoherent scattering from the Klein-Nishina formula corrected for binding effects. In the second column incoherent scattering is given by the Klein-Nishina formula for free electrons.

b Barns/atom x 0.05016 = cm^2/g

* Energy region in which dipole absorption attains a maximum cross section.

TABLE 15. Nitrogen

Photon energy	Scattering[a]		Photoelectric K and L shells	Pair production		Total[b]	
	With coherent	Without coherent		Nucleus	Electron	With coherent	Without coherent
Mev	Barns/atom	Barns/atom	Barns/atom	Barns/atom	Barns/atom	cm^2/g	cm^2/g
0.01	8.96	4.48	79.4			3.80	3.61
.015	6.72	4.40	21.2			1.20	1.10
.02	5.73	4.33	8.21			0.600	0.539
.03	4.84	4.18	2.15			.301	.272
.04	4.45	4.05	0.81			.226	.209
.05	4.14	3.93	.38			.194	.185
.06	3.98	3.82	.21			.180	.173
.08	3.73	3.62	.082			.164	.159
.10	3.54	3.45	.041			.154	.150
.15	3.15	3.11	.010			.136	.134
.20	2.87	2.85				.123	.123
.30	2.48	2.47				.107	.106
.40		2.22					.0955
.50		2.02					.0869
.60		1.872					.0805
.80		1.645					.0707
1.0		1.478					.0636
1.5		1.201		.0022			.0517
2.0		1.025		.0086			.0445
3.0		0.806		.025	0.00009		.0357
4.0		.672		.040	.0003		.0306
5.0		.580		.054	.0008		.0273
6.0		.512		.066	.001		.0249
8.0		.419		.086	.003		.0218
10		.357		.103	.004		.0200
15		.264		.134	.008		.0175
20		.212		.158	.010		.0163
30		.1539		.190	.015		.0154‡
40		.1222		.213	.018		.0152
50		.1019		.231	.020		.0152
60		.0878		.244	.023		.0153
80		.0692		.264	.026		.0154
100		.0574		.280	.029		.0158

a Data in the first column is given by the sum of coherent scattering and of incoherent scattering from the Klein-Nishina formula corrected for binding effects. In the second column incoherent scattering is given by the Klein-Nishina formula for free electrons.

b Barns/atom x 0.04301 = cm^2/g

‡ Energy region in which dipole absorption attains a maximum cross section.

TABLE 16. Oxygen

Photon energy	Scattering[a]		Photoelectric K and L shells	Pair production		Total[b]	
	With coherent	Without coherent		Nucleus	Electron	With coherent	Without coherent
Mev	Barns/atom	Barns/atom	Barns/atom	Barns/atom	Barns/atom	cm^2/g	cm^2/g
0.01	11.5	5.12	146			5.93	5.69
.015	8.28	5.03	39.6			1.80	1.68
.02	6.95	4.94	15.4			0.842	0.766
.03	5.77	4.78	4.09			.371	.334
.04	5.18	4.62	1.55			.253	.232
.05	4.80	4.49	0.73			.208	.197
.06	4.61	4.37	.40			.189	.180
.08	4.30	4.14	.15			.168	.162
.10	4.06	3.94	.071			.156	.151
.15	3.61	3.55	.020			.137	.134
.20	3.29	3.25	.010			.124	.123
.30	2.84	2.83				.107	.107
.40	2.54	2.53				.0956	.0953
.50		2.31					.0870
.60		2.14					.0806
.80		1.880					.0708
1.0		1.690					.0636
1.5		1.373		0.0028			.0518
2.0		1.171		.011			.0445
3.0		0.921		.032	0.0001		.0359
4.0		.768		.053	.0004		.0309
5.0		.663		.070	.0009		.0276
6.0		.586		.086	.002		.0254
8.0		.479		.112	.003		.0224
10		.408		.134	.005		.0206
15		.302		.175	.009		.0183
20		.242		.206	.012		.0173‡
30		.1759		.248	.017		.0166
40		.1397		.278	.021		.0165
50		.1165		.300	.023		.0165
60		.1003		.317	.026		.0167
80		.0790		.344	.030		.0171
100		.0656		.364	.034		.0175

a Data in the first column is given by the sum of coherent scattering and of incoherent scattering from the Klein-Nishina formula corrected for binding effects. In the second column incoherent scattering is given by the Klein-Nishina formula for free electrons.

b Barns/atom x 0.03765 = cm^2/g

‡ Energy region in which dipole absorption attains a maximum cross section.

TABLE 17. Sodium

Photon energy	Scattering[a]		Photoelectric K,L and M shells	Pair production		Total[b]	
	With coherent	Without coherent		Nucleus	Electron	With coherent	Without coherent
Mev	Barns/atom	Barns/atom	Barns/atom	Barns/atom	Barns/atom	cm^2/g	cm^2/g
0.01	20	7.04	588			15.9	15.6
.015	14	6.92	169			4.80	4.61
.02	11.2	6.80	67.5			2.06	1.95
.03	8.8	6.57	18.1			0.705	0.646
.04	7.8	6.36	7.0			.388	.350
.05	7.1	6.17	3.3			.273	.248
.06	6.67	6.01	1.87			.224	.206
.08	6.08	5.69	0.74			.179	.168
.10	5.70	5.42	.35			.159	.151
.15	5.01	4.88	.091			.134	.130
.20	4.54	4.47	.040			.120	.118
.30	3.92	3.89	.010			.103	.102
.40	3.50	3.48				.0917	.0912
.50	3.19	3.18				.0836	.0833
.60		2.94					.0770
.80		2.58					.0676
1.0		2.32					.0608
1.5		1.888		0.0054			.0496
2.0		1.610		.021			.0427
3.0		1.266		.061	0.0001		.0348
4.0		1.056		.100	.0005		.0303
5.0		0.911		.133	.001		.0274
6.0		.805		.163	.002		.0254
8.0		.659		.211	.004		.0229
10		.561		.252	.007		.0215
15		.415		.330	.012		.0198
20		.333		.387	.016		.0193
30		.242		.465	.023		.0191
40		.1921		.521	.028		.0194
50		.1602		.562	.032		.0198
60		.1379		.595	.036		.0201
80		.1087		.645	.041		.0208
100		.0901		.680	.046		.0214

a Data in the first column is given by the sum of coherent scattering and of incoherent scattering from the Klein-Nishina formula corrected for binding effects. In the second column incoherent scattering is given by the Klein-Nishina formula for free electrons.

b Barns/atom x 0.02620 = cm^2/g

TABLE 18. Magnesium

Photon energy	Scattering[a]		Photoelectric K,L and M shells	Pair production		Total[b]	
	With coherent	Without coherent		Nucleus	Electron	With coherent	Without coherent
Mev	Barns/atom	Barns/atom	Barns/atom	Barns/atom	Barns/atom	cm^2/g	cm^2/g
0.01	25	7.68	847			21.6	21.2
.015	17	7.55	246			6.51	6.28
.02	13	7.42	99.7			2.79	2.65
.03	10.2	7.16	27.2			0.926	0.851
.04	8.7	6.94	10.6			.478	.434
.05	7.9	6.73	5.1			.322	.293
.06	7.4	6.55	2.8			.253	.232
.08	6.66	6.20	1.11			.192	.181
.10	6.24	5.91	0.53			.168	.160
.15	5.48	5.32	.14			.139	.135
.20	4.97	4.88	.060			.125	.122
.30	4.28	4.24	.020			.107	.106
.40	3.82	3.80	.010			.0949	.0944
.50	3.48	3.47				.0862	.0860
.60		3.21					.0795
.80		2.82					.0699
1.0		2.53					.0627
1.5		2.06		0.0064			.0512
2.0		1.797		.026			.0442
3.0		1.381		.073	0.0001		.0360
4.0		1.152		.119	.0006		.0315
5.0		0.994		.159	.001		.0286
6.0		.878		.194	.002		.0266
8.0		.719		.251	.005		.0242
10		.612		.300	.007		.0228
15		.463		.393	.013		.0213
20		.363		.459	.018		.0208
30		.264		.553	.025		.0209
40		.210		.619	.031		.0213
50		.1747		.667	.035		.0217
60		.1505		.707	.039		.0222
80		.1185		.765	.045		.0230
100		.0983		.807	.050		.0237

a Data in the first column is given by the sum of coherent scattering and of incoherent scattering from the Klein-Nishina formula corrected for binding effects. In the second column incoherent scattering is given by the Klein-Nishina formula for free electrons.

b Barns/atom x 0.02477 = cm^2/g

TABLE 19. Aluminum

Photon energy	Scattering[a]		Photoelectric K,L and M shells	Pair production		Total[b]	
	With coherent	Without coherent		Nucleus	Electron	With coherent	Without coherent
Mev	Barns/atom	Barns/atom	Barns/atom	Barns/atom	Barns/atom	cm^2/g	cm^2/g
0.01	.29	8.32	1170			26.8	26.3
.015	19	8.18	343			8.08	7.84
.02	15	8.03	141			3.48	3.33
.03	11.5	7.76	39.0			1.13	1.04
.04	9.8	7.51	15.2			0.558	0.507
.05	8.8	7.29	7.3			.360	.326
.06	8.1	7.10	4.0			.270	.248
.08	7.26	6.72	1.61			.198	.186
.10	6.79	6.41	0.78			.169	.161
.15	5.96	5.77	.21			.138	.134
.20	5.39	5.29	.080			.122	.120
.30	4.64	4.60	.020			.104	.103
.40	4.14	4.12	.010			.0927	.0922
.50	3.78	3.76				.0844	.0840
.60	3.49	3.48				.0779	.0777
.80		3.06					.0683
1.0		2.75					.0614
1.5		2.23		0.0076			.0500
2.0		1.903		.030			.0432
3.0		1.496		.086	0.0002		.0353
4.0		1.247		.140	.0006		.0310
5.0		1.077		.186	.001		.0282
6.0		0.952		.227	.002		.0264
8.0		.778		.295	.005		.0241
10		.663		.353	.008		.0229
15		.490		.460	.014		.0215
20		.393		.539	.019		.0212*
30		.286		.647	.027		.0214
40		.227		.726	.033		.0220
50		.1893		.782	.038		.0225
60		.1630		.828	.042		.0231
80		.1284		.896	.049		.0240
100		.1065		.944	.055		.0247

a Data in the first column is given by the sum of coherent scattering and of incoherent scattering from the Klein-Nishina formula corrected for binding effects. In the second column incoherent scattering is given by the Klein-Nishina formula for free electrons.

b Barns/atom x 0.02233 = cm^2/g

* Energy region in which dipole absorption attains a maximum cross section.

TABLE 20. Silicon

Photon energy	Scattering[a]		Photoelectric K,L and M shells	Pair production		Total[b]	
	With coherent	Without coherent		Nucleus	Electron	With coherent	Without coherent
Mev	Barns/atom	Barns/atom	Barns/atom	Barns/atom	Barns/atom	cm^2/g	cm^2/g
0.01	33	8.96	1580			34.6	34.1
.015	22	8.81	470			10.6	10.3
.02	17	8.65	194			4.53	4.35
.03	12.8	8.36	54.4			1.44	1.35
.04	10.8	8.09	21.4			0.691	0.633
.05	9.7	7.85	10.3			.429	.389
.06	8.9	7.64	5.8			.315	.288
.08	8.0	7.24	2.3			.221	.205
.10	7.38	6.90	1.11			.182	.172
.15	6.44	6.21	0.29			.144	.139
.20	5.82	5.69	.12			.127	.125
.30	5.01	4.95	.040			.108	.107
.40	4.46	4.43	.020			.0961	.0954
.50	4.07	4.05				.0873	.0869
.60	3.75	3.74				.0804	.0802
.80	3.30	3.29				.0708	.0706
1.0		2.96					.0635
1.5		2.40		0.0088			.0517
2.0		2.05		.035			.0447
3.0		1.611		.100	0.0002		.0367
4.0		1.343		.162	.0007		.0323
5.0		1.160		.216	.002		.0296
6.0		1.025		.264	.003		.0277
8.0		0.838		.342	.006		.0254
10		.714		.408	.009		.0243
15		.528		.533	.015		.0231
20		.423		.623	.021		.0229‡
30		.308		.749	.029		.0233
40		.244		.838	.036		.0240
50		.204		.904	.041		.0246
60		.1756		.957	.046		.0253
80		.1383		1.03	.053		.0262
100		.1147		1.09	.059		.0271

a Data in the first column is given by the sum of coherent scattering and of incoherent scattering from the Klein-Nishina formula corrected for binding effects. In the second column incoherent scattering is given by the Klein-Nishina formula for free electrons.

b Barns/atom x 0.02145 = cm^2/g

‡ Energy region in which dipole absorption attains a maximum cross section.

TABLE 21. Phosphorus

Photon energy	Scattering[a]		Photoelectric K,L and M shells	Pair production		Total[b]	
	With coherent	Without coherent		Nucleus	Electron	With coherent	Without coherent
Mev	Barns/atom	Barns/atom	Barns/atom	Barns/atom	Barns/atom	cm^2/g	cm^2/g
0.01	38	9.60	2090			41.4	40.8
.015	25	9.44	619			12.5	12.2
.02	19	9.27	259			5.41	5.22
.03	14.3	8.96	74.3			1.72	1.62
.04	12.0	8.67	28.8			0.794	0.729
.05	10.6	8.42	13.8			.475	.432
.06	9.7	8.19	7.8			.340	.311
.08	8.6	7.76	3.1			.228	.211
.10	7.98	7.39	1.55			.185	.174
.15	6.93	6.65	0.40			.143	.137
.20	6.26	6.10	.17			.125	.122
.30	5.37	5.30	.05			.105	.104
.40	4.79	4.75	.02			.0936	.0928
.50	4.36	4.34	.01			.0850	.0846
.60	4.02	4.01				.0782	.0780
.80	3.53	3.52				.0687	.0685
1.0		3.17					.0617
1.5		2.57		0.010			.0502
2.0		2.20		.040			.0436
3.0		1.726		.114	0.0002		.0358
4.0		1.439		.186	.0007		.0316
5.0		1.243		.248	.002		.0290
6.0		1.096		.302	.003		.0273
8.0		0.898		.393	.006		.0252
10		.765		.469	.009		.0242
15		.566		.610	.016		.0232
20		.454		.714	.022		.0231
30		.330		.858	.031		.0237
40		.262		.961	.038		.0245
50		.218		1.03	.044		.0251
60		.1861		1.10	.049		.0260
80		.1482		1.19	.056		.0271
100		.1229		1.25	.063		.0279

a Data in the first column is given by the sum of coherent scattering and of incoherent scattering from the Klein-Nishina formula corrected for binding effects. In the second column incoherent scattering is given by the Klein-Nishina formula for free electrons.

b Barns/atom x 0.01945 = cm^2/g

TABLE 22. Sulphur

Photon energy	Scattering[a]		Photoelectric K,L and M shells	Pair production		Total[b]	
	With coherent	Without coherent		Nucleus	Electron	With coherent	Without coherent
Mev	Barns/atom	Barns/atom	Barns/atom	Barns/atom	Barns/atom	cm^2/g	cm^2/g
0.01	44	10.24	2700			51.6	50.9
.015	29	10.06	820			16.0	15.6
.02	22	9.89	344			6.88	6.65
.03	15.9	9.55	98.7			2.15	2.03
.04	13.2	9.25	38.5			0.971	0.897
.05	11.6	8.98	18.6			.567	.518
.06	10.7	8.74	10.6			.400	.363
.08	9.3	8.27	4.2			.254	.234
.10	8.6	7.89	2.1			.201	.188
.15	7.49	7.10	0.57			.150	.144
.20	6.69	6.51	.23			.130	.127
.30	5.74	5.66	.070			.109	.108
.40	5.12	5.07	.030			.0968	.0958
.50	4.66	4.63	.020			.0879	.0874
.60	4.30	4.28	.010			.0810	.0806
.80	3.77	3.76				.0708	.0707
1.0	3.39	3.38				.0637	.0635
1.5		2.75		0.012			.0519
2.0		2.34		.046			.0448
3.0		1.842		.13	0.0002		.0971
4.0		1.535		.21	.0008		.0328
5.0		1.325		.28	.002		.0302
6.0		1.171		.34	.003		.0284
8.0		0.958		.45	.006		.0266
10		.816		.53	.010		.0255
15		.604		.69	.017		.0246
20		.484		.81	.023		.0247
30		.352		.98	.033		.0256
40		.279		1.09	.041		.0265
50		.233		1.18	.047		.0274
60		.201		1.24	.052		.0281
80		.1580		1.34	.060		.0293
100		.1311		1.42	.067		.0304

a Data in the first column is given by the sum of coherent scattering and of incoherent scattering from the Klein-Nishina formula corrected for binding effects. In the second column incoherent scattering is given by the Klein-Nishina formula for free electrons.

b Barns/atom x 0.01879 = cm^2/g

TABLE 29. Argon

Photon energy	Scattering[a]		Photoelectric K,L and M shells	Pair production		Total[b]	
	With coherent	Without coherent		Nucleus	Electron	With coherent	Without coherent
Mev	Barns/atom	Barns/atom	Barns/atom	Barns/atom	Barns/atom	cm^2/g	cm^2/g
0.01	56	11.52	4280			65.4	64.7
.015	36	11.32	1320			20.5	20.1
.02	28	11.12	561			8.88	8.63
.03	19	10.75	164			2.76	2.64
.04	15.8	10.40	64.5			1.21	1.13
.05	13.6	10.10	31.6			0.682	0.629
.06	12.4	9.89	18.0			.459	.420
.08	10.8	9.31	7.2			.271	.249
.10	9.85	8.87	3.6			.203	.188
.15	8.43	7.98	0.98			.142	.135
.20	7.57	7.32	.41			.120	.117
.30	6.48	6.36	.12			.0995	.0977
.40	5.76	5.70	.050			.0876	.0867
.50	5.24	5.21	.030			.0795	.0790
.60	4.84	4.82	.020			.0733	.0730
.80	4.24	4.23				.0640	.0638
1.0	3.81	3.80				.0575	.0573
1.5		3.09		0.015			.0468
2.0		2.64		.058			.0407
3.0		2.07		.17	0.0002		.0338
4.0		1.727		.27	.0009		.0301
5.0		1.491		.36	.002		.0279
6.0		1.318		.44	.003		.0266
8.0		1.078		.56	.007		.0248
10		0.918		.67	.011		.0241
15		.679		.87	.019		.0237
20		.544		1.02	.026		.0240
30		.396		1.23	.037		.0251
40		.314		1.37	.046		.0261
50		.262		1.48	.053		.0271
60		.226		1.57	.059		.0280
80		.1778		1.69	.068		.0292
100		.1475		1.78	.076		.0302

a Data in the first column is given by the sum of coherent scattering and of incoherent scattering from the Klein-Nishina formula corrected for binding effects. In the second column incoherent scattering is given by the Klein-Nishina formula for free electrons.

b Barns/atom x 0.01506 = cm^2/g

TABLE 24. Potassium

Photon energy	Scattering[a]		Photoelectric K,L and M shells	Pair production		Total[b]	
	With coherent	Without coherent		Nucleus	Electron	With coherent	Without coherent
Mev	Barns/atom	Barns/atom	Barns/atom	Barns/atom	Barns/atom	cm^2/g	cm^2/g
0.01	63	12.16	5260			82.0	81.2
.015	40	11.95	1650			26.0	25.6
.02	31	11.74	698			11.2	10.9
.03	21	11.34	206			3.50	3.35
.04	17.1	10.98	81.5			1.52	1.43
.05	14.7	10.66	40.1			0.844	0.782
.06	13.3	10.37	23.0			.559	.514
.08	11.6	9.82	9.2			.321	.293
.10	10.5	9.37	4.6			.233	.215
.15	8.95	8.43	1.27			.157	.149
.20	8.02	7.73	0.52			.132	.127
.30	6.85	6.72	.15			.108	.106
.40	6.09	6.02	.070			.0949	.0938
.50	5.53	5.49	.040			.0858	.0852
.60	5.11	5.08	.020			.0791	.0786
.80	4.48	4.46	.010			.0692	.0689
1.0	4.02	4.01				.0619	.0618
1.5		3.26		0.017			.0505
2.0		2.78		.065			.0438
3.0		2.19		.18	0.0002		.0365
4.0		1.823		.30	.0009		.0327
5.0		1.574		.40	.002		.0305
6.0		1.391		.48	.004		.0289
8.0		1.138		.63	.008		.0274
10		0.969		.75	.012		.0267
15		.717		.97	.020		.0263
20		.575		1.14	.028		.0269
30		.418		1.37	.040		.0282
40		.332		1.53	.049		.0294
50		.277		1.65	.056		.0306
60		.238		1.74	.062		.0314
80		.1877		1.88	.072		.0330
100		.1557		1.98	.080		.0341

a Data in the first column is given by the sum of coherent scattering and of incoherent scattering from the Klein-Nishina formula corrected for binding effects. In the second column incoherent scattering is given by the Klein-Nishina formula for free electrons.

b Barns/atom x 0.01541 = cm^2/g

TABLE 25. Calcium

Photon energy	Scattering[a]		Photoelectric K,L and M shells	Pair production		Total[b]	
	With coherent	Without coherent		Nucleus	Electron	With coherent	Without coherent
Mev	Barns/atom	Barns/atom	Barns/atom	Barns/atom	Barns/atom	cm^2/g	cm^2/g
0.01	69	12.80	6380			96.9	96.1
.015	44	12.58	2010			30.9	30.4
.02	33	12.36	859			13.4	13.1
.03	23	11.94	254			4.16	4.00
.04	18.5	11.56	102			1.81	1.71
.05	15.8	11.22	50.6			0.998	0.929
.06	14.3	10.92	28.8			.648	.597
.08	12.3	10.34	11.6			.359	.330
.10	11.1	9.86	6.0			.257	.238
.15	9.48	8.87	1.63			.167	.158
.20	8.47	8.13	0.67			.137	.132
.30	7.23	7.07	.20			.112	.109
.40	6.42	6.33	.090			.0979	.0965
.50	5.84	5.78	.050			.0885	.0876
.60	5.38	5.35	.030			.0813	.0809
.80	4.72	4.70	.010			.0711	.0708
1.0	4.24	4.22				.0637	.0634
1.5		3.43		0.018			.0518
2.0		2.98		.072			.0451
3.0		2.30		.20	0.0002		.0376
4.0		1.919		.33	.0009		.0338
5.0		1.657		.44	.002		.0316
6.0		1.464		.54	.004		.0302
8.0		1.198		.69	.008		.0285
10		1.020		.83	.012		.0280
15		0.755		1.08	.022		.0279
20		.605		1.26	.029		.0285*
30		.440		1.51	.042		.0299
40		.349		1.69	.051		.0314
50		.291		1.82	.059		.0326
60		.251		1.93	.065		.0338
80		.198		2.08	.075		.0354
100		.1639		2.19	.084		.0366

a Data in the first column is given by the sum of coherent scattering and of incoherent scattering from the Klein-Nishina formula corrected for binding effects. In the second column incoherent scattering is given by the Klein-Nishina formula for free electrons.

b Barns/atom x 0.01503 = cm^2/g

* Energy region in which dipole absorption attains a maximum cross section.

TABLE 26. Iron

Photon energy	Scattering[a]		Photoelectric K,L and M shells	Pair production		Total[b]	
	With coherent	Without coherent		Nucleus	Electron	With coherent	Without coherent
Mev	Barns/atom	Barns/atom	Barns/atom	Barns/atom	Barns/atom	cm^2/g	cm^2/g
0.01	120	16.64	16500			179	178
.015	75	16.35	5380			58.8	58.2
.02	55	16.07	2380			26.3	25.8
.03	37	15.52	729			8.26	8.03
.04	29	15.03	308			3.64	3.48
.05	24	14.59	155			1.93	1.83
.06	20.7	14.20	91			1.20	1.13
.08	17.2	13.44	38			0.595	0.555
.10	15.4	12.82	19.1			.372	.344
.15	12.8	11.53	5.4			.196	.183
.20	11.3	10.57	2.23			.146	.138
.30	9.50	9.19	0.66			.110	.106
.40	8.42	8.23	.29			.0940	.0919
.50	7.63	7.52	.16			.0840	.0828
.60	7.03	6.96	.10			.0769	.0762
.80	6.15	6.11	.05			.0669	.0664
1.0	5.52	5.49	.03			.0599	.0595
1.5		4.46		0.032			.0485
2.0		3.81		.12			.0424
3.0		2.99		.35	0.0903		.0360
4.0		2.50		.56	.001		.0330
5.0		2.15		.75	.003		.0313
6.0		1.903		.91	.005		.0304
8.0		1.597		1.17	.011		.0295
10		1.326		1.39	.016		.0294
15		0.981		1.81	.028		.0304
20		.786		2.10	.038		.0315*
30		.572		2.52	.054		.0339
40		.454		2.81	.067		.0359
50		.379		3.03	.076		.0376
60		.326		3.21	.085		.0391
80		.257		3.46	.098		.0412
100		.213		3.64	.11		.0427

a Data in the first column is given by the sum of coherent scattering and of incoherent scattering from the Klein-Nishina formula corrected for binding effects. In the second column incoherent scattering is given by the Klein-Nishina formula for free electrons.

b Barns/atom x 0.01079 = cm^2/g

* Energy region in which dipole absorption attains a maximum cross section.

TABLE 27. Copper

Photon energy	Scattering[a]		Photoelectric K,L and M shells	Pair production		Total[b]	
	With coherent	Without coherent		Nucleus	Electron	With coherent	Without coherent
Mev	Barns/atom	Barns/atom	Barns/atom	Barns/atom	Barns/atom	cm^2/g	cm^2/g
0.01	150	18.56	23600			225	224
.015	96	18.24	8000			76.8	76.0
.02	70	17.92	3580			34.6	34.1
.03	46	17.31	1120			11.1	10.8
.04	35	16.76	474			4.83	4.65
.05	28	16.27	242			2.56	2.45
.06	24	15.83	143			1.58	1.51
.08	20.2	14.99	60.2			0.762	0.713
.10	17.9	14.29	30.7			.461	.427
.15	14.5	12.86	8.9			.222	.206
.20	12.8	11.79	3.7			.156	.147
.30	10.7	10.25	1.1			.112	.108
.40	9.43	9.18	0.48			.0940	.0916
.50	8.54	8.39	.26			.0834	.0820
.60	7.86	7.76	.16			.0760	.0751
.80	6.87	6.82	.08			.0659	.0654
1.0	6.16	6.12	.05			.0589	.0585
1.5		4.98		0.041			.0476
2.0		4.25		.16			.0418
3.0		3.34		.43	0.0004		.0357
4.0		2.78		.70	.001		.0330
5.0		2.40		.93	.003		.0316
6.0		2.123		1.13	.006		.0309
8.0		1.736		1.45	.012		.0303
10		1.479		1.72	.018		.0305
15		1.094		2.23	.031		.0318
20		0.877		2.60	.043		.0334*
30		.638		3.12	.060		.0362
40		.506		3.48	.074		.0385
50		.422		3.75	.085		.0404
60		.364		3.97	.094		.0420
80		.286		4.27	.11		.0442
100		.238		4.49	.12		.0460

a Data in the first column is given by the sum of coherent scattering and of incoherent scattering from the Klein-Nishina formula corrected for binding effects. In the second column incoherent scattering is given by the Klein-Nishina formula for free electrons.

b Barns/atom x 0.009482 = cm^2/g

* Energy region in which dipole absorption attains a maximum cross section.

TABLE 28. Molybdenum

Photon energy	Scattering[a]		Photoelectric K,L and M shells	Pair production		Total[b]	
	With coherent	Without coherent		Nucleus	Electron	With coherent	Without coherent
Mev	Barns/atom	Barns/atom	Barns/atom	Barns/atom	Barns/atom	cm^2/g	cm^2/g
0.01	340	26.9	11400			73.7	71.8
.015	220	26.4	3480			23.2	22.0
.0200[c]	160	26.0	1510			10.5	9.64
.0200	160	26.0	13000			82.6	81.8
.03	98	25.1	4260			27.4	26.9
.04	71	24.3	1920			12.5	12.2
.05	56	23.6	1030			6.82	6.62
.06	46	22.9	620			4.18	4.04
.08	36	21.7	274			1.95	1.86
.10	30	20.7	144			1.09	1.03
.15	23.2	18.63	43.4			0.418	0.389
.20	19.8	17.08	18.7			.242	.225
.30	16.1	14.85	5.8			.138	.130
.40	14.0	13.30	2.6			.104	.0998
.50	12.6	12.15	1.4			.0879	.0851
.60	11.5	11.24	0.88			.0777	.0761
.80	10.0	9.87	.45			.0656	.0648
1.0	8.96	8.87	.29			.0581	.0575
1.5	7.25	7.21	.14	0.095		.0470	.0467
2.0		6.15	.09	.35			.0414
3.0		4.83	.05	.93	0.0005		.0365
4.0		4.03	.04	1.49	.002		.0349
5.0		3.48	.03	1.96	.005		.0344
6.0		3.08	.023	2.36	.008		.0344
8.0		2.52	.017	3.00	.02		.0349
10		2.14	.013	3.53	.03		.0359
15		1.585		4.58	.04		.0390‡
20		1.270		5.32	.06		.0418
30		0.924		6.39	.09		.0465
40		.733		7.11	.11		.0499
50		.612		7.65	.12		.0526
60		.527		8.08	.14		.0549
80		.415		8.69	.16		.0582
100		.344		9.15	.18		.0607

a Data in the first column is given by the sum of coherent scattering and of incoherent scattering from the Klein-Nishina formula corrected for binding effects. In the second column incoherent scattering is given by the Klein-Nishina formula for free electrons.

b Barns/atom x 0.006279 = cm^2/g

c K edge; at this and lower energies data for the L and M shells is given while at this and higher energies data for the L, M and K shells is given.

‡ Energy region in which dipole absorption attains a maximum cross section.

TABLE 29. Tin

Photon energy	Scattering[a]		Photoelectric K,L and M shells	Pair production		Total[b]	
	With coherent	Without coherent		Nucleus	Electron	With coherent	Without coherent
Mev	Barns/atom	Barns/atom	Barns/atom	Barns/atom	Barns/atom	cm^2/g	cm^2/g
0.01	510	32.0	24000			124	122
.015	340	31.4	7410			39.3	37.8
.02	240	30.9	3220			17.6	16.5
.02925[c]	150	30.0	1050			6.09	5.48
.02925	150	30.0	8580			44.3	43.7
.03	140	29.8	8150			42.1	41.5
.04	100	28.9	3700			19.3	18.9
.05	79	28.0	1990			10.5	10.2
.06	65	27.3	1210			6.47	6.28
.08	49	25.8	539			2.98	2.87
.10	40	24.6	286			1.65	1.58
.15	29.6	22.2	88.8			0.601	0.563
.20	24.6	20.3	39.3			.324	.309
.30	19.7	17.68	12.4			.163	.159
.40	17.0	15.84	5.6			.115	.109
.50	15.2	14.46	3.0			.0924	.0886
.60	13.8	13.38	1.9			.0797	.0776
.80	12.0	11.75	1.0			.0660	.0647
1.0	10.7	10.56	0.64			.0576	.0568
1.5	8.65	8.58	.32	0.14		.0462	.0459
2.0	7.36	7.32	.20	.51		.0410	.0408
3.0		5.76	.12	1.35	0.0006		.0367
4.0		4.80	.08	2.12	.002		.0355
5.0		4.14	.06	2.78	.006		.0355
6.0		3.66	.05	3.33	.01		.0358
8.0		2.99	.04	4.20	.02		.0368
10		2.55	.03	4.94	.03		.0383
15		1.886	.02	6.39	.05		.0424
20		1.512	.015	7.40	.07		.0457
30		1.100		8.91	.10		.0513
40		0.873		9.89	.13		.0553
50		.728		10.6	.15		.0583
60		.627		11.2	.16		.0609
80		.494		12.1	.19		.0649
100		.410		12.7	.21		.0676

a Data in the first column is given by the sum of coherent scattering and of incoherent scattering from the Klein-Nishina formula corrected for binding effects. In the second column incoherent scattering is given by the Klein-Nishina formula for free electrons.

b Barns/atom x 0.005076 = cm^2/g

c K edge; at this and lower energies data for the L and M shells is given while at this and higher energies data for the L, M and K shells is given.

TABLE 30. Iodine

Photon energy	Scattering[a]		Photoelectric K,L and M shells	Pair production		Total[b]	
	With coherent	Without coherent		Nucleus	Electron	With coherent	Without coherent
Mev	Barns/atom	Barns/atom	Barns/atom	Barns/atom	Barns/atom	cm^2/g	cm^2/g
0.01	590	33.9	29800			144	142
.015	380	33.3	9360			46.2	44.6
.02	270	32.8	4130			20.9	19.8
.03	160	31.6	1260			6.74	6.13
.03323[c]	150	31.3	933			5.14	4.58
.03323[c]	150	31.3	7510			36.4	35.8
.04	120	30.6	4490			21.9	21.5
.05	89	29.7	2470			12.1	11.9
.06	72	28.9	1500			7.46	7.26
.08	54	27.4	677			3.47	3.34
.10	44	26.1	360			1.92	1.83
.15	32	23.5	113			0.688	0.648
.20	26.5	21.5	50			.363	.339
.30	21.0	18.74	16.0			.176	.165
.40	18.1	16.78	7.2			.120	.114
.50	16.2	15.33	3.9			.0954	.0913
.60	14.8	14.18	2.5			.0821	.0792
.80	12.8	12.46	1.3			.0669	.0653
1.0	11.4	11.19	0.84			.0581	.0571
1.5	9.18	9.10	.41	0.17		.0463	.0460
2.0	7.81	7.76	.26	.59		.0411	.0409
3.0		6.10	.16	1.53	0.0006		.0370
4.0		5.09	.11	2.39	.003		.0360
5.0		4.39	.08	3.12	.006		.0361
6.0		3.88	.07	3.72	.01		.0365
8.0		3.17	.05	4.70	.02		.0377
10		2.70	.04	5.52	.03		.0394
15		2.00	.03	7.12	.06		.0437‡
20		1.603	.02	8.26	.08		.0473
30		1.165		9.92	.11		.0592
40		0.925		11.0	.14		.0673
50		.772		11.9	.16		.0609
60		.665		12.5	.17		.0633
80		.524		13.5	.20		.0675
100		.434		14.1	.22		.0700

a Data in the first column is given by the sum of coherent scattering and of incoherent scattering from the Klein-Nishina formula corrected for binding effects. In the second column incoherent scattering is given by the Klein-Nishina formula for free electrons.

b Barns/atom x 0.00167 = cm^2/g

c K edge; at this and lower energies data for the L and M shells is given while at this and higher energies data for the L, M and K shells is given.

‡ Energy region in which dipole absorption attains a maximum cross section.

TABLE 31. Tungsten

Photon energy	Scattering[a]		Photoelectric K,L and M shells	Pair production		Total[b]	
	With coherent	Without coherent		Nucleus	Electron	With coherent	Without coherent
Mev	Barns/atom	Barns/atom	Barns/atom	Barns/atom	Barns/atom	cm^2/g	cm^2/g
0.01	1300	47.4	17700			62.2	58.1
.01022[c]	1200	47.3	16800			59.0	55.2
.01212[d]	1000	46.9	64700			215	212
.015	840	46.5	36000			121	118
.02	590	45.7	16000			54.3	52.6
.03	350	44.2	5040			17.7	16.7
.04	240	42.8	2220			8.06	7.41
.05	180	41.5	1160			4.39	3.94
.06	145	40.4	674			2.68	2.34
.06964[e]	122	39.4	437			1.83	1.56
.06964	122	39.4	3230			11.0	10.7
.08	104	38.3	2250			7.71	7.49
.10	80	36.5	1250			4.36	4.21
.15	54	32.8	408			1.51	1.44
.20	42	30.1	186			0.747	0.708
.30	31.5	26.2	63.1			.310	.293
.40	26.5	23.4	29.8			.184	.174
.50	23.4	21.4	16.7			.131	.125
.60	21.2	19.80	11.0			.105	.101
.80	18.2	17.39	5.9			.0789	.0763
1.0	16.1	15.63	3.9			.0655	.0640
1.5	12.9	12.70	1.9	0.41		.0498	.0492
2.0	10.9	10.83	1.2	1.32		.0440	.0437
3.0	8.57	8.52	0.71	3.13	0.0009	.0407	.0405
4.0		7.10	.50	4.68	.004		.0402
5.0		6.13	.38	5.96	.006		.0409
6.0		5.42	.31	7.02	.01		.0418
8.0		4.43	.23	8.68	.03		.0438
10		3.77	.18	10.2	.04		.0465
15		2.79	.11	13.1	.08		.0527
20		2.24	.08	15.2	.11		.0578
30		1.627	.06	18.3	.15		.0660
40		1.292	.04	20.3	.19		.0715
50		1.077		21.8	.22		.0757
60		0.928		23.1	.24		.0795
80		.731		24.8	.28		.0845
100		.606		26.1	.31		.0885

a Data in the first column is given by the sum of coherent scattering and of incoherent scattering from the Klein-Nishina formula corrected for binding effects. In the second column incoherent scattering is given by the Klein-Nishina formula for free electrons.

b Barns/atom x 0.003276 = cm^2/g

c L_3 edge; at this and lower energies data for the M shell is given.

d L_1 edge; from this energy to the K edge energy data for the L and M shells is given.

e K edge; at this and higher energies data for the L, M and K shells is given.

TABLE 32. Platinum

Photon energy	Scattering[a]		Photoelectric K,L and M shells	Pair production		Total[b]	
	With coherent	Without coherent		Nucleus	Electron	With coherent	Without coherent
Mev	Barns/atom	Barns/atom	Barns/atom	Barns/atom	Barns/atom	cm^2/g	cm^2/g
0.01	1400	49.9	22000			72.2	68.0
.01158[c]	1200	49.6	14800			49.4	45.8
.01391[d]	1000	49.2	53900			169	166
.015	940	49.1	43800			138	135
.02	670	48.2	19700			62.9	60.9
.03	400	46.6	6240			20.5	19.4
.04	280	45.1	2720			9.26	8.53
.05	210	43.8	1440			5.09	4.58
.06	163	42.6	836			3.08	2.71
.07858[e]	117	40.6	380			1.53	1.30
.07858[e]	117	40.6	2860			9.19	8.95
.08	115	40.3	2750			8.84	8.61
.10	88	38.4	1500			4.90	4.75
.15	59	34.6	498			1.72	1.64
.20	45	31.7	226			0.836	0.795
.30	34	27.6	77.3			.343	.324
.40	28.3	24.7	37.1			.202	.191
.50	24.8	22.6	21.2			.142	.135
.60	22.5	20.9	13.9			.112	.107
.80	19.2	18.33	7.6			.0827	.0800
1.0	17.0	16.47	4.9			.0676	.0659
1.5	13.6	13.38	2.4	0.47		.0508	.0501
2.0	11.6	11.42	1.5	1.51		.0451	.0445
3.0	9.04	8.98	0.90	3.52	0.001	.0415	.0414
4.0	7.52	7.48	.63	5.21	.004	.0412	.0411
5.0		6.46	.48	6.59	.009		.0418
6.0		5.71	.39	7.73	.02		.0427
8.0		4.67	.29	9.54	.03		.0448
10		3.98	.22	11.2	.05		.0477
15		2.94	.14	14.4	.08		.0542
20		2.36	.10	16.7	.11		.0595
30		1.715	.07	20.1	.16		.0680
40		1.362	.06	22.3	.20		.0738
50		1.136	.04	24.0	.23		.0784
60		0.978		25.4	.25		.0822
80		.770		27.3	.29		.0875
100		.639		28.6	.33		.0913

a Data in the first column is given by the sum of coherent scattering and of incoherent scattering from the Klein-Nishina formula corrected for binding effects. In the second column incoherent scattering is given by the Klein-Nishina formula for free electrons.

b Barns/atom x 0.003086 = cm^2/g

c L_3 edge; at this and lower energies data for the M shell is given.

d L_1 edge; from this energy to the K edge energy data for the L and M shells is given.

e K edge; at this and higher energies data for the L, M and K shells is given.

TABLE 33. Thallium

Photon energy	Scattering[a]		Photoelectric K,L and M shells	Pair production		Total[b]	
	With coherent	Without coherent		Nucleus	Electron	With coherent	Without coherent
Mev	Barns/atom	Barns/atom	Barns/atom	Barns/atom	Barns/atom	cm^2/g	cm^2/g
0.01	1500	51.8	26000			81.1	76.8
.01268[c]	1200	51.3	13400			43.0	39.7
.01537[d]	990	50.7	47200			142	139
.02	730	50.1	22700			69.1	67.1
.03	430	48.4	7220			22.6	21.4
.04	300	46.8	3200			10.3	9.57
.05	220	45.4	1660			5.54	5.03
.06	180	44.2	976			3.41	3.01
.08	124	41.9	420			1.60	1.36
.08584[e]	114	41.3	341			1.34	1.13
.08584[e]	114	41.3	2577			7.93	7.72
.10	95	39.9	1710			5.32	5.16
.15	63	35.9	576			1.88	1.80
.20	48	32.9	261			0.911	0.866
.30	35.5	28.6	88.9			.367	.346
.40	29.6	25.6	43.6			.216	.204
.50	26.0	23.4	25.0			.150	.143
.60	23.4	21.7	16.4			.117	.112
.80	20.0	19.04	8.9			.0852	.0824
1.0	17.8	17.11	5.8			.0696	.0675
1.5	14.2	13.90	2.8	0.53		.0517	.0508
2.0	12.0	11.86	1.8	1.67		.0456	.0452
3.0	9.40	9.32	1.1	3.83	0.001	.0422	.0420
4.0	7.81	7.77	0.72	5.62	.004	.0417	.0416
5.0		6.71	.56	7.08	.009		.0423
6.0		5.93	.45	8.29	.02		.0433
8.0		4.85	.32	10.2	.03		.0454
10		4.13	.25	12.0	.05		.0484
15		3.06	.17	15.4	.09		.0552
20		2.45	.12	17.9	.12		.0607
30		1.781	.09	21.5	.17		.0694
40		1.414	.07	23.9	.21		.0754
50		1.179	.05	25.7	.24		.0801
60		1.016		27.1	.26		.0837
80		0.800		29.2	.31		.0894
100		.664		30.6	.34		.0932

a Data in the first column is given by the sum of coherent scattering and of incoherent scattering from the Klein-Nishina formula corrected for binding effects. In the second column incoherent scattering is given by the Klein-Nishina formula for free electrons.

b Barns/atom x 0.002948 = cm^2/g

c L_3 edge; at this and lower energies data for the M shell is given.

d L_1 edge; from this energy to the K edge energy data for the L and M shells is given.

e K edge; at this and higher energies data for the L, M and K shells is given.

TABLE 34. Lead

Photon energy	Scattering[a]		Photoelectric K,L and M shells	Pair production		Total[b]	
	With coherent	Without coherent		Nucleus	Electron	With coherent	Without coherent
Mev	Barns/atom	Barns/atom	Barns/atom	Barns/atom	Barns/atom	cm^2/g	cm^2/g
0.01	1600	52.5	27500			84.6	80.1
.01307[c]	1200	51.8	13200			41.9	38.5
.01589[d]	980	51.3	45400			135	132
.02	750	50.7	24000			72.0	69.9
.03	450	49.0	7620			23.5	22.3
.04	310	47.4	3310			10.5	9.76
.05	230	46.0	1740			5.73	5.19
.06	180	44.8	1040			3.55	3.15
.08	1[illegible]	42.4	444			1.66	1.41
.08823[e]	1[illegible]	41.6	334			1.30	1.09
.08823[e]	113	41.6	2510			7.63	7.42
.10	100	40.4	1780			5.47	5.29
.15	64	36.4	596			1.92	1.84
.20	49	33.3	275			0.942	0.896
.30	36.2	29.0	93.4			.377	.356
.40	30.1	26.0	45.7			.220	.208
.50	26.3	23.7	26.1			.152	.145
.60	23.8	21.9	17.3			.119	.114
.80	20.3	19.27	9.5			.0866	.0836
1.0	18.0	17.32	6.2			.0704	.0684
1.5	14.4	14.07	3.0	0.55		.0522	.0512
2.0	12.2	12.00	2.0	1.72		.0463	.0457
3.0	9.51	9.44	1.1	3.93	0.001	.0423	.0421
4.0	7.91	7.87	0.80	5.76	.004	.0421	.0420
5.0		6.79	.60	7.25	.009		.0426
6.0		6.00	.49	8.47	.02		.0436
8.0		4.91	.35	10.5	.03		.0459
10		4.18	.28	12.3	.05		.0489
15		3.09	.18	15.7	.09		.0554*
20		2.48	.13	18.3	.12		.0611
30		1.803	.09	21.9	.17		.0697
40		1.432	.07	24.4	.21		.0759
50		1.194	.05	26.2	.24		.0805
60		1.028		27.7	.27		.0843
80		0.810		29.8	.31		.0899
100		.672		31.3	.34		.0939

a Data in the first column is given by the sum of coherent scattering and of incoherent scattering from the Klein-Nishina formula corrected for binding effects. In the second column incoherent scattering is given by the Klein-Nishina formula for free electrons.

b Barns/atom x 0.002908 = cm^2/g

c L_3 edge; at this and lower energies data for the M shell is given.

d L_1 edge; from this energy to the K edge energy data for the L and M shells is given.

e K edge; at this and higher energies data for the L, M and K shells is given.

* Energy region in which dipole absorption attains a maximum cross section.

TABLE 35. Uranium

Photon energy	Scattering[a]		Photoelectric K,L and M shells	Pair production		Total[b]	
	With coherent	Without coherent		Nucleus	Electron	With coherent	Without coherent
Mev	Barns/atom	Barns/atom	Barns/atom	Barns/atom	Barns/atom	cm^2/g	cm^2/g
0.01	2100	58.9	44600			118	113
.015	1400	57.9	14500			40.2	36.8
.01720[c]	1200	57.4	10000			28.3	25.5
.02181[d]	880	56.5	29400			76.6	74.6
.03	590	54.9	12000			31.9	30.5
.04	400	53.2	5250			14.3	13.4
.05	300	51.6	2780			7.79	7.17
.06	230	50.2	1640			4.73	4.28
.08	163	47.6	716			2.22	1.93
.10	123	45.3	374			1.26	1.06
.1163[e]	103	43.8	239			0.865	0.716
.1163[e]	103	43.8	1790			4.79	4.64
.15	78	40.8	916			2.52	2.42
.20	59	37.4	425			1.22	1.17
.30	42	32.5	146			0.476	0.452
.40	34.7	29.1	73.2			.273	.259
.50	30.2	26.6	43.1			.185	.176
.60	27.1	24.6	29.2			.142	.136
.80	23.0	21.6	16.0			.0987	.0952
1.0	20.3	19.43	10.5			.0779	.0757
1.5	16.2	15.79	5.1	0.77		.0559	.0548
2.0	13.7	13.47	3.3	2.35		.0490	.0484
3.0	10.7	10.59	1.9	5.09	0.001	.0448	.0445
4.0	8.88	8.83	1.3	7.26	.004	.0441	.0440
5.0		7.62	1.0	9.00	.01		.0446
6.0		6.74	0.81	10.4	.02		.0455
8.0		5.51	.59	12.8	.04		.0479
10		4.69	.46	15.0	.06		.0511
15		3.47	.30	19.3	.10		.0586‡
20		2.78	.22	22.4	.13		.0646
30		2.023	.15	26.8	.19		.0738
40		1.606	.11	29.8	.24		.0804
50		1.340	.09	32.1	.27		.0855
60		1.154		33.9	.30		.0895
80		0.909		36.5	.35		.0956
100		.754		38.3	.39		.0998

a Data in the first column is given by the sum of coherent scattering and of incoherent scattering from the Klein-Nishina formula corrected for binding effects. In the second column incoherent scattering is given by the Klein-Nishina formula for free electrons.

b Barns/atom x 0.002531 = cm^2/g

c L_3 edge; at this and lower energies only M shell data is given.

d L_1 edge; from this to the K edge energy data for the L and M shells is given.

e K edge; at this and higher energies data for the L, M and K shells is given.

‡ Energy region in which dipole absorption attains a maximum cross section.

TABLE 36. Water

Photon energy	Scattering[a]		Photoelectric K and L shells	Pair production		Total[b]	
	With coherent	Without coherent		Nucleus	Electron	With coherent	Without coherent
Mev	Barns/molecule	Barns/molecule	Barns/molecule	Barns/molecule	Barns/molecule	cm^2/g	cm^2/g
0.01	12.8	6.40	146			5.31	5.10
.015	9.54	6.29	39.6			1.64	1.53
.02	8.19	6.18	15.4			0.789	0.722
.03	6.96	5.97	4.09			.370	.336
.04	6.34	5.78	1.55			.264	.245
.05	5.92	5.61	0.73			.222	.212
.06	5.70	5.46	.40			.204	.196
.08	5.33	5.17	.15			.183	.178
.10	5.05	4.93	.071			.171	.167
.15	4.50	4.44	.020			.151	.149
.20	4.10	4.07	.010			.137	.136
.30	3.55	3.54				.119	.118
.40		3.17					.106
.50		2.89					.0966
.60		2.68					.0896
.80		2.35					.0786
1.0		2.11					.0706
1.5		1.716		0.0029			.0575
2.0		1.464		.011			.0493
3.0		1.151		.033	0.0001		.0396
4.0		0.960		.055	.0004		.0339
5.0		.828		.072	.001		.0301
6.0		.732		.089	.002		.0275
8.0		.599		.116	.003		.0240
10		.510		.138	.006		.0219
15		.377		.181	.010		.0190
20		.302		.213	.014		.0177
30		.220		.256	.019		.0166
40		.1746		.287	.024		.0162
50		.1456		.310	.026		.0161
60		.1254		.327	.029		.0161
80		.0988		.355	.034		.0163
100		.0820		.376	.038		.0166

a Data in the first column is given by the sum of coherent scattering and of incoherent scattering from the Klein-Nishina formula corrected for binding effects. In the second column incoherent scattering is given by the Klein-Nishina formula for free electrons.

b Barns/molecule x 0.033144 = cm^2/g

TABLE 37. Sodium Iodide

Photon energy	Scattering[a]		Photoelectric K,L and M shells	Pair production		Total[b]	
	With coherent	Without coherent		Nucleus	Electron	With coherent	Without coherent
Mev	Barns/molecule	Barns/molecule	Barns/molecule	Barns/molecule	Barns/molecule	cm^2/g	cm^2/g
0.01	610	41.0	30400			125	122
.015	390	40.3	9530			39.9	38.5
.02	280	39.6	4200			18.0	17.0
.03	170	38.2	1280			5.83	5.30
.03323[c]	160	37.8	946			4.45	3.95
.03323	160	37.8	7520			30.9	30.4
.04	130	37.0	4500			18.6	18.2
.05	96	35.9	2470			10.3	10.1
.06	79	34.9	1500			6.35	6.17
.08	60	33.1	678			2.97	2.86
.10	50	31.5	360			1.65	1.57
.15	37	28.4	113			0.603	0.568
.20	31	26.0	50.0			.326	.305
.30	24.9	22.6	16.0			.164	.155
.40	21.6	20.3	7.2			.116	.111
.50	19.4	18.51	3.9			.0936	.0901
.60	17.7	17.12	2.5			.0812	.0789
.80	15.4	15.04	1.3			.0671	.0657
1.0	13.7	13.52	0.84			.0584	.0577
1.5	11.1	10.98	.41	0.18		.0470	.0465
2.0	9.42	9.37	.26	.61		.0414	.0412
3.0		7.37	.16	1.59	0.0007		.0367
4.0		6.14	.11	2.49	.004		.0351
5.0		5.30	.08	3.25	.007		.0347
6.0		4.68	.07	3.88	.01		.0347
8.0		3.83	.05	4.91	.02		.0354
10		3.26	.04	5.77	.04		.0366
15		2.41	.03	7.45	.07		.0400
20		1.935	.02	8.65	.10		.0430
30		1.407		10.4	.13		.0480
40		1.117		11.5	.17		.0514
50		0.932		12.5	.19		.0547
60		.803		13.1	.21		.0567
80		.632		14.1	.24		.0602
100		.525		14.8	.27		.0627

a Data in the first column is given by the sum of coherent scattering and of incoherent scattering from the Klein-Nishina formula corrected for binding effects. In the second column incoherent scattering is given by the Klein-Nishina formula for free electrons.

b Barns/molecule x 0.004019 = cm^2/g

c K-edge of Iodine; at this and lower energies data for the L and M shells is given while at this and higher energies data for the L, M and K shells is given.

TABLE 38. Calcium Phosphate

Photon energy	Scattering[a]		Photoelectric K,L and M shells	Pair production		Total[b]	
	With coherent	Without coherent		Nucleus	Electron	With coherent	Without coherent
Mev	Barns/molecule	Barns/molecule	Barns/molecule	Barns/molecule	Barns/molecule	cm^2/g	cm^2/g
0.01	375	98.6	24500			48.3	47.8
.015	248	96.9	7580			15.2	14.9
.02	193	95.2	3220			6.63	6.44
.03	144	91.9	943			2.11	2.01
.04	121	89.0	376			0.965	0.903
.05	107	86.4	185			.567	.527
.06	99.2	84.1	105			.397	.367
.08	88.5	79.6	42.2			.254	.237
.10	81.7	75.9	21.7			.201	.190
.15	71.2	68.3	5.84			.150	.144
.20	64.2	62.6	2.41			.129	.126
.30	55.2	54.4	0.72			.109	.107
.40	49.2	48.8	.32			.0962	.0954
.50	44.7	44.5	.18			.0872	.0868
.60	41.3	41.2	.11			.0804	.0802
.80	36.3	36.2	.05			.0706	.0704
1.0	32.6	32.5	.03			.0634	.0632
1.5		26.4		0.10			.0515
2.0		22.5		.38			.0444
3.0		17.73		1.08	0.002		.0346
4.0		14.78		1.79	.007		.0322
5.0		12.75		2.38	.02		.0294
6.0		11.27		2.91	.03		.0276
8.0		9.22		3.75	.06		.0253
10		7.85		4.50	.09		.0242
15		5.81		5.86	.17		.0230
20		4.66		6.86	.23		.0228
30		3.39		8.23	.32		.0232
40		2.69		9.22	.40		.0239
50		2.24		9.92	.45		.0245
60		1.931		10.5	.50		.0251
80		1.522		11.4	.58		.0262
100		1.263		12.0	.65		.0270

a Data in the first column is given by the sum of coherent scattering and of incoherent scattering from the Klein-Nishina formula corrected for binding effects. In the second column incoherent scattering is given by the Klein-Nishina formula for free electrons.

b Barns/molecule x 0.001942 = cm^2/g

TABLE 39. Air

0.755 N, 0.232 O, 0.013 A by Weight

Mass Absorption Coefficient

Photon energy	Total With coherent	Total Without coherent	Photon energy	Total With coherent	Total Without coherent
Mev	cm^2/g	cm^2/g	Mev	cm^2/g	cm^2/g
0.01	5.09	4.89	1.0	.0635	.0635
.015	1.59	1.48	1.5		.0517
.02	0.764	0.697	2.0		.0445
.03	.349	.317	3.0		.0357
.04	.245	.226	4.0		.0307
.05	.204	.194	5.0		.0274
.06	.186	.178	6.0		.0250
.08	.166	.161	8.0		.0220
.10	.155	.151	10		.0202
.15	.136	.134	15		.0178
.20	.123	.123	20		.0166
.30	.107	.106	30		.0158
.40	.0954	.0953	40		.0156
.50	.0868	.0868	50		.0157
.60	.0804	.0804	60		.0158
.80	.0706	.0706	80		.0160
			100		.0164

Table 40. Concrete

(0.56% H, 49.56% O, 31.35% Si, 4.56% Al, 8.26% Ca, 1.22% Fe, 0.21% Mg, 1.71% Na, 1.92% K, 0.12% S) (ρ = 2.35 g/cm^3)

Photon energy	Mass Absorption Coefficient	Photon energy	Mass Absorption Coefficient	Photon energy	Mass Absorption Coefficient
Mev	cm^2/g	Mev	cm^2/g	Mev	cm^2/g
0.01	24.6	.30	.107	6.0	.0268
.015	7.68	.40	.0954	8.0	.0243
.02	3.34	.50	.0870	10.0	.0229
.03	1.10	.60	.0804	15	.0214
.04	.542	.80	.0706	20	.0209
.05	.350	1.0	.0635	30	.0209
.06	.267	1.5	0.0517	40	.0213
.08	.197	2.0	.0445	50	.0217
.10	.169	3.0	.0363	60	.0222
.15	.139	4.0	.0317	80	.0230
.20	.124	5.0	.0287	100	.0237

Coherent scattering is not included in the calculations. The data were not revised.

TABLE 41. *Incoherent scattering function, S(v)*

$v=\frac{qa}{3\hbar Z^{1/3}}$	Thomas-Fermi[a]	Lenz[b]	Koppe[c]	$v=\frac{qa}{3\hbar Z^{1/3}}$	Thomas-Fermi[a]	Lenz[b]	Koppe[c]
0.001	0.012	0.0068	0.00037	0.3	0.776	0.890	.....
.005	.051	.....	.....	.4	.839	.....	.....
.01	.097	.074	.024	.5	.880	.995	0.828
.02	.169	.....	.....	.6	.909	.....	.....
.03	.227	.217	.....	.7	.929	.....	.....
.04	.277	.....	.....	.8	.944	.....	.....
.05	.319	.....	.196	.9	.954	.....	.....
.1	.486	.560	.370	1.0	.962	1.0	.934
.2	.674	.....	.583				

[a] Values below $v=0.05$ are from Wheeler and Lamb, and from $v=0.05$ to 1 from Bewilogua.
[b] Values are calculated for the Molière approximation to the Thomas-Fermi distribution.
[c] Values are calculated for analytical interpolation to give correct values at low v and Thomas-Fermi at high v.

5. Appendix—Survey of Data on the Incoherent Scattering Function

Many effects of the interaction of radiations with atoms depend on the so-called incoherent scattering function $S(q,Z)$. Among these are the small-angle incoherent scattering of X-rays [73], the small-angle inelastic scattering of charged particles [74, 75], and the production of bremsstrahlung and of positron-electron pairs in the field of electrons [76]. Data on $S(q,Z)$ are represented in the graphs of figures 6 and 7 and in table 41.

The incoherent scattering function represents the probability that an atom of a specified material be raised to any excited or ionized state as a result of a sudden impulsive action which imparts a recoil momentum $\vec{q}$ to any of the atomic electrons.

The generalized form factor of an atom with atomic number Z can be defined as a matrix element

$$F_\epsilon(\vec{q})=\left(\epsilon\left|\sum_{j=1}^{Z} e^{\frac{i\vec{q}\cdot\vec{r}_j}{\hbar}}\right|0\right), \tag{15}$$

where $\vec{r}_j$ is the position vector of the jth electron with respect to the nucleus, and ϵ indicates the energy of an excited (or ionized) stationary state, as measured from the ground state. The expression (15) and all of its applications in this appendix have been derived and should be considered only in the frame of nonrelativistic quantum mechanics.

The incoherent scattering function $S(q,Z)$ is the sum of the $|F_\epsilon(\vec{q})|^2$ over-all excited states of the atom, divided by the number of electrons, Z. The sum is independent of the direction of $\vec{q}$ for atoms with spherical symmetry or for an assembly of atoms with random orientation.

In order to minimize the variation of the incoherent scattering function from one element to another it is convenient to express the recoil momentum q in terms of a suitable unit, namely, to replace q by the variable

$$v=0.333\ qa/\hbar Z^{2/3}, \tag{16}$$

where $a=0.53\times10^{-8}$ cm is the Bohr radius.

The incoherent scattering function is then indicated as

$$S(v)=S(0.333\ qa/\hbar Z^{2/3})=(1/Z)\int_{\epsilon>0}^{\infty} d\epsilon|F_\epsilon(\vec{q})|^2 \tag{17}$$

where the integral includes both a sum over the discrete spectrum and an integral over the continuous spectrum. The function (17) still depends on Z at constant v, but this dependence is not indicated explicitly.

This equation may be transformed by application of a closure theorem (sum rule) so that it defines $S(v)$ in terms of properties of the ground state only, specifically in terms of diagonal elements of matrices pertaining to the ground state

$$S(v)=(1/Z)[(0\|\sum_j e^{\frac{i\vec{q}\cdot\vec{r}_j}{\hbar}}|^2|0)-|F(\vec{q},Z)|^2] \tag{18}$$

where F(q,Z) is the form factor that determines the coherent scattering.

When the electron recoil momentum, q, is much larger than the initial momentum of the electron in its bound state, the electric forces that initially

were binding the electron in the atom influence the recoil only to a slight extent. The recoiling electron is practically certain to leave the atom, and the incoherent scattering function is very nearly equal to 1. This feature is displayed by every graph in figure 6. On the other hand, if the recoil momentum is very small, the atom is almost certain to absorb the recoil as though it were a rigid body, that is, to remain in its ground state. Accordingly, $S(v)$ tends to vanish for small values of v, as shown in figure 6.

Hydrogen atom. The incoherent scattering function for the hydrogen atom can be calculated analytically, because the H wave function is known analytically, and has in fact a simple algebraic form. The first term in the bracket of eq (18) equals 1 for H and the second term equals

$$[1+q^2a^2/4\hbar^2]^{-4}=[1+9.04v^2/4]^{-4}.$$

Therefore,

$$S(v)=1-[1+9.04v^2/4]^{-4}$$
$$=\frac{(9.04v^2/4)(2+9.04v^2/4)(2+9.04v^2/2+81.6v^4/16)}{(1+9.04v^2/4)^4}. \quad (19)$$

This expression is plotted in figure 6.

Thomas-Fermi model. The incoherent scattering function for an atom described by the Thomas-Fermi model has been calculated by Heisenberg [77] and Bewilogua [78]. According to this model the incoherent scattering function, $S(v)$, is a universal function independent of Z, i. e., valid for all elements. It is plotted in figure 6 and tabulated in table 41. It was stated by the authors that this application of the Thomas-Fermi model should be valid for $Z>6$, on the basis of comparison with calculations for C and O atoms with screened hydrogenic wave functions.

The Thomas-Fermi model yields an electron distribution that is excessively smeared out at the edge of the atom. This causes the incoherent scattering function to be in error for small values of v. The incorrect assumption that this part of the electronic distribution is spread out with low density, low binding energy, and low momentum yields an erroneously large probability of incoherent scattering with low recoil momentum. Therefore, the Thomas-Fermi $S(v)$ tapers off much too slowly for low v, that is, on the left side of figure 6.

The Thomas-Fermi model also gives an incorrectly high density of electrons near the nucleus, as though there were a portion of the electronic charge with excessively high momentum. There results an incorrectly large probability of coherent scattering for comparatively large values of q and v, and a corresponding incorrectly low probability of incoherent scattering. As a result the Thomas-Fermi $S(v)$ approaches 1 in the region of $v=1$ too gradually. This is indicated by the comparison of the Thomas-Fermi $S(v)$ with the curves calculated from the Hartree model in figure 7.

Lenz [79] has suggested that simplified calculations be made utilizing the approximate formula for the electron density of the Thomas-Fermi atom introduced by Molière [80]. In table 41 a comparison is made of $S(v)$ obtained by Bewilogua for the Thomas-Fermi model and values from the Molière type of approximation. The Molière distribution of electrons drops off at the edge of the atom faster, and therefore more realistically, than the Thomas-Fermi distribution. Accordingly the scattering function is more in line with realistic expectation than is the original Bewilogua curve.

Low-v approximation. Koppe [81] has suggested that the incoherent scattering function be calculated, for low v, from an improved model. For low v, that is for low q, the exponential in eq (15) can be expanded into powers of q, disregarding powers after the first. The first term of the expansion, namely $\sum_j 1=Z$, contributes to $F_\epsilon(q)$ an amount $Z(\epsilon|1|0)$, which vanishes owing to the orthogonality of the eigenfunctions. The next term yields

$$F_\epsilon(\vec{q})\sim\frac{i\vec{q}}{\hbar}\cdot\sum_j(\epsilon|\vec{r}_j|0). \quad (20)$$

This expression vanishes for parity reasons when $\epsilon=0$. A closure theorem yields then

$$S(v)=(1/Z)\int_0^\infty|F_\epsilon(\vec{q})|^2d\epsilon\sim\frac{1}{Z}\left(0\left|\left[\frac{\vec{q}\cdot\sum_j\vec{r}_j}{\hbar}\right]^2\right|0\right)$$
$$=\frac{1}{Z}\frac{q^2}{3\hbar^2}(0|\sum_j\vec{r}_j|^2|0), \quad (21)$$

where the last equality has been obtained by averaging over-all directions of $\vec{q}$ and taking into account the assumed spherical symmetry of the atom.

Because the atomic electrons move very nearly independently of one another, the square of $\sum_j\vec{r}_j$ in eq (21) has an average value nearly equal to that of $\sum_j|\vec{r}_j|^2$. This latter average can be obtained for various substances from experimental values of the volume diamagnetic susceptibility χ_{dia} according to the law that

$$(0|\sum_j|\vec{r}_j|^2|0)=\frac{1}{N}\frac{6\,mc^2}{e^2}(-\chi_{dia})$$
$$=1.25\times10^6(-\chi_{dia})\frac{A}{\rho}a^2, \quad (22)$$

where N is the number of atoms per cubic centimeter, A is the atomic numper, ρ the density in

grams per cubic centimeter, and a is the Bohr radius. Equation (22) differs from Koppe's eq (14) by a factor of 2. This discrepancy is probably due to an inconsistency between the normalizations involved in the various equations [81, p. 661].

A reasonable approach to obtain a complete curve $S(v)$ would be to draw $S(v)$ for low v on the basis of eq (21) and (22), for large v on the basis of the Thomas-Fermi curve, and then join by interpolation the parts of the curve thus obtained. Koppe has suggested that this interpolation be done simply by multiplying the Thomas-Fermi $S(v)$ by the factor $v/(v+A)$, where the constant A is adjusted to yield the correct behavior for low v. However, this interpolation formula appears to give values of $S(v)$ that are too low for intermediate values of v (see table 41). Therefore, a more realistic interpolation seems necessary.

Hartree model calculations. A more basic approach to the calculation of $S(q, Z)$ utilizes electron atoms provided by the Hartree self-consistent field method [82]. Data obtained by this method are discussed in this section, but on the whole, applications of the Hartree method to the incoherent scattering function appear much less advanced than one might believe.

The Hartree method starts from an independent particle picture, which assumes that the excitation or ionization involves one electron only, leaving the other electrons undisturbed. From this standpoint the incoherent scattering function for a material represents simply an average of the incoherent scattering functions for its separate electrons. One can then write

$$S(q,Z)=1-(1/Z)\sum_i|f_0^{(i)}(q)|^2, \qquad (23)$$

where $f_0^{(i)}(q)$ indicates the probability that the ith electron gets neither excited nor detached, even though it has received the recoil momentum q. The quantity $f_0^{(i)}(q)$ is not quite the same as the ordinary form factor $f^{(i)}(q)$, which represents the contribution of the ith electron to coherent scattering; the difference lies in the fact that the excitation of an electron from one orbit to another may be forbidden by the exclusion principle.

Data on the form factor $f^{(i)}(q)$ for electrons in a few orbits and for a number of atoms have been provided by James and Brindley [47] on the basis of Hartree wave functions. Values of $\epsilon|f^{(i)}(q)|^2$ have been calculated from these data by Compton and Allison [83]. However, it is not clear how this data was obtained for the higher Z materials because James and Brindley give practically no data for shells higher than the M shell. The combined difference between $|f_0^{(i)}(\vec{q})|^2$ and $|f^{(i)}(\vec{q})|^2$ for all electrons is treated by Waller and Hartree [84] and indicated as a corrective term by Pirenne [74]. The relative importance of this corrective term decreases as the number of electrons in the atom increases.

Calculations including the correction of Waller–Hartree have been made for neon and argon [84,85]. In a limited region of the variable v the values of $S(v)$ thus obtained are in good agreement with values from the Thomas-Fermi model (see fig. 7).

Wentzel model. Lenz [74] suggested that one assume a distribution of the electronic charge within the atom according to a model introduced by Wentzel. With this model a constant can be adjusted so as to yield the experimental value of the diamagnetic susceptibility, which implies a correct behavior for $S(v)$ at low v. This procedure implies really that the atom behaves with respect to incoherent scattering as though it contained a single charged particle distributed in density as described by the Wentzel formula [86]. This density is

$$\rho=\frac{Z}{4\pi r R^2}e^{-r/R}, \qquad (24)$$

where

$$R=\sqrt{\frac{(0|\sum_j|\vec{r}_j|^2|0)}{6Z}} \qquad (25)$$

then

$$S(v)=1-\left[\frac{1}{(1+q^2R^2/\hbar^2)^2}\right]=\frac{(q^2R^2/\hbar^2)(2+q^2R^2/\hbar^2)}{(1+q^2R^2/\hbar^2)^2}$$

$$=\left\{1-\frac{1}{\left[1+9.04Z^{1/3}v^2\left(-1.25\times10^6\chi_{d1a}\frac{A}{\rho}\right)\frac{1}{6Z}\right]^2}\right\}. \qquad (26)$$

Curves according to eq (26) for Pb and C (graphite) are plotted in figure 6.

It is difficult to assess the accuracy provided by the Wentzel model. The density (24), being singular at $r=0$, should yield an excessively slow approach of $S(v)$ to 1 as v increases. In practice $S(v)$ approaches 1 for lower values of v than in other models but this is presumably due to more serious inaccuracies of the model at medium distances from the nucleus.

Conclusion. The preceding discussion indicates that existing approximate models fail to yield accurate data on the incoherent scattering function. Under the circumstances the values of $S(q,Z)$ derived from the Thomas-Fermi model were used, because the final results did not appear to depend critically on the systematic errors of these values for low and large q.

6. References

[1] U. Fano, Nucleonics **11**, 8 (1953); **11**, 55 (1953).
[2] H. A. Bethe and J. Ashkin, Experimental nuclear physics, **I**, part II, E. Segrè, editor (John Wiley & Sons, Inc., New York, N. Y., 1953).
[3] C. M. Davisson and R. D. Evans, Revs. Mod. Phys. **24**, 102 (1952).
[4] G. T. P. Tarrant, Proc. Cambridge Phil. Soc. **28**, 475 (1932).
[5] S. A. Colgate, Phys. Rev. **87**, 592 (1952).
[6] P. Debye, Physik. Z. **31**, 419 (1930).
[7] W. Franz, Physik. Z. **98**, 314 (1935).
[8] P. B. Moon, Proc. Phys. Soc. (London) [A] **63**, 1189 (1950).
[9] A. Sommerfeld, Atombau and Spektrallinien **II**, 436 (F. Vieweg und Sohn, Braunschweig, 1939).
[10] H. Hall, Revs. Mod. Phys. **8**, 358 (1936).
[11] H. A. Bethe and L. C. Maximon, Phys. Rev. **93**, 768 (1954).
[12] W. Heitler, The quantum theory of radiation, 3d ed., p. 207 (Oxford University Press, Amen House, London E. C. 4, 1954).
[13] F. Sauter, Ann. Physik **11**, 454 (1931); ibid. **9**, 217 (1931).
[14] M. Stobbe, Ann. Physik **7**, 661 (1930).
[15] H. R. Hulme, Proc. Roy. Soc. (London) [A] **133**, 381 (1931); also H. R. Hulme, J. McDougall, R. A. Buckingham, and R. H. Fowler, Proc. Roy. Soc. (London) [A] **149**, 131 (1935).
[16] H. Hall, Phys. Rev. **45**, 620 (1934).
[17] F. G. Nagasaka (Thesis, Notre Dame Univ., Indiana, Aug. 1955).
[18] G. D. Latyshev, Revs. Mod. Phys. **19**, 132 (1947).
[19] J. C. Slater, Phys. Rev. **36**, 57 (1930).
[20] A. T. Nelms, NBS Circ. 542 (1952).
[21] D. E. Lea, Actions of radiations on living cells, p. 347 (Cambridge Univ. Press, Cambridge); also (MacMillan Co., N. Y., 1943).
[22] A. T. Nelms and I. Oppenheim, J. Research NBS **55**, 53 (1955) RP2604.
[23] H. A. Bethe and W. Heitler, Proc. Roy. Soc. (London) [A] **146**, 83 (1934).
[24] F. Sauter, Ann. Physik **20**, 404 (1934).
[25] G. Racah, Nuovo cimento **11**, 461 (1934).
[26] H. A. Bethe, Proc. Cambridge Phil. Soc. **30**, 524 (1934).
[27] J. A. Wheeler and W. E. Lamb, Jr., Phys. Rev. **55**, 858 (1939).
[28] J. C. Jaeger and H. R. Hulme, Proc. Roy. Soc. (London) [A] **153**, 443 (1936).
[29] J. C. Jaeger, Nature **137**, 731 (1936); ibid. **148**, 86 (1941).
[30] H. Davies, H. A. Bethe, and L. C. Maximon, Phys. Rev. **93**, 788 (1954).
[31] A. Borsellino, Helv. Phys. Acta **20**, 136 (1947); Nuovo cimento **4**, 112 (1947).
[32] V. Vortruba, Phys. Rev. **73**, 1468 (1948); Bul. intern. acad. tchèque sci., Prague **49**, 19 (1948).
[33] F. Rohrlich and J. Joseph, Bul. Am. Phys. Soc. **30**, No. 7 (1955); Phys. Rev. **100**, 1241 (1955).
[34] D. Bernstein and W. K. H. Panofsky, Phys. Rev. **102**, 522 (1956).
[35] P. Nemirovsky, J. Phys. (U. S. S. R.) **11**, 94 (1947).
[36] K. M. Watson, Phys. Rev. **72**, 1060 (1947).
[37] R. Montalbetti, L. Katz, and J. Goldernberg, Phys. Rev. **91**, 659 (1953).
[38] R. Nathans and J. Halpern, Phys. Rev. **93**, 437 (1954).
[39] E. G. Fuller and E. Hayward, Phys. Rev. **101**, 692 (1956).
[40] M. N. Lewis (informal communication).
[41] M. T. Jones, Phys. Rev. **50**, 110 (1936).
[42] T. R. Cuykendall, Phys. Rev. **50**, 105 (1936).
[43] K. W. Seemann, Bul. Am. Phys. Soc. **1**, 198, NA8 (1956).
[44] S. J. M. Allen, Phys. Rev. **28**, 907 (1926).
[45] K. Grosskurth, Ann. Physik **20**, 197 (1934).
[46] J. Victoreen, J. Appl. Phys. **14**, 95 (1943); **19**, 855 (1948); **20**, 1141 (1949).
[47] R. W. James and G. W. Brindley, Phil. Mag. **12**, 81 (1931).
[48] A. H. Compton and S. K. Allison, X-rays in theory and experiment (D. van Nostrand Co., Inc., New York, N. Y., 1935).
[49] H. Hönl, Ann. Physik **18**, 625 (1933); Z. Physik **84**, 1 (1933).
[50] L. G. Parratt and C. F. Hempstead, Phys. Rev. **94**, 1593 (1954).
[51] J. L. Burkhardt, Phys. Rev. **100**, 192 (1955); R. R. Wilson, Phys. Rev. **82**, 295 (1951).
[52] A. Storruste, Proc. Phys. Soc. (London) [A] **63**, 1197 (1950).
[53] A. K. Mann, Phys. Rev. **101**, 4 (1956).
[54] P. V. C. Hough, Phys. Rev. **73**, 266 (1948).
[55] I. E. Dayton, Phys. Rev. **89**, 544 (1953).
[56] B. Hahn, E. Baldinger, and P. Huber, Helv. Phys. Acta **25**, 505 (1952).
[57] P. Schmid and P. Huber, Helv. Phys. Acta **27**, 152 (1954).
[58] P. Schmid, Absolute Paarbildungsquerschnitte von Blei für Gammastrahlen von Co^{60} und Na^{24} und Paarerzeugung der RaC-Gamma-Strahlung in Blei (Thesis, Basel Univ., 1955).
[59] R. S. Paul, Phys. Rev. **96**, 1563 (1954).
[60] E. S. Rosenblum, E. F. Shrader, and R. M. Warner, Jr., Phys. Rev. **88**, 612 (1952).
[61] H. I. West, Jr., Phys. Rev. **101**, 915 (1956).
[62] J. D. Anderson, R. W. Kenney, C. A. McKonald, Jr., and R. F. Past, Phys. Rev. **102**, 1632 (1956).
[63] R. L. Walker, Phys. Rev. **76**, 527 (1949).
[64] S. A. Colgate, Phys. Rev. **76**, 1440 (1949).
[65] A. I. Berman, Phys. Rev. **90**, 210 (1953).
[66] J. L. Lawson, Phys. Rev. **75**, 433 (1949).
[67] J. W. Dewire, A. Ashkin, and L. A. Beach, Phys. Rev. **83**, 505 (1951).
[68] G. D. Adams, Phys. Rev. **74**, 1707 (1948).
[69] C. L. Cowan, Phys. Rev. **74**, 1841 (1948).
[70] P. E. Argyle, Can. J. Phys. **29**, 83 (1951).
[71] J. J. Wyard, Phys. Rev. **87**, 165 (1952); Proc. Phys. Soc. (London) [A] **66**, 382 (1953).
[72] P. R. Howland and W. E. Kreger, Phys. Rev. **95**, 407 (1954).
[73] A. H. Compton, Phys. Rev. **21**, 483 (1923); P. Debye, Physik. Z. **24**, 161 (1923); I. Waller, Phil. Mag. **4**, 1228 (1927); Z. Physik **51**, 213 (1928); G. Wentzel, Z. Physik **43**, 1, 779 (1927).
[74] P. M. Morse, Physik Z. **33**, 443 (1932); M. H. Pirenne, The diffraction of X rays and electrons by free molecules (Cambridge University Press, 1946); F. Lentz, Naturwiss **39**, 265 (1952); Z. Naturforsch **9a**, 185–204 (1954).
[75] U. Fano, Phys. Rev. **93**, 117 (1954).
[76] H. Bethe, Proc. Cambridge Phil. Soc. **30**, 524 (1934).
[77] W. Heisenberg, Physik. Z. **32**, 737 (1931).
[78] L. Bewilogua, Physik. Z. **32**, 740 (1931). Values of $S(v)$ for $v<0.05$ are given by Wheeler and Lamb, ref. [27].
[79] F. Lenz, Z. Physik **135**, 248 (1953).
[80] G. Molière, Z. Naturforsch **2a**, 133 (1947).
[81] H. Koppe, Z. Physik **124**, 658 (1947).
[82] D. R. Hartree, Repts. Progr. Phys. **11**, 113 (1946-47). A Summary of Hartree wave-function calculations is included in this paper. J. C. Slater, Phys. Rev. **81**, 385 (1951); G. W. Pratt, Jr., Phys. Rev. **88**, 1217 (1952); R. E. Meyerott, Argonne Nat. Lab. Rep. 5008 (March, 1953).
[83] A. H. Compton and S. K. Allison, X-rays in theory and practice, p. 782 (D. Van Nostrand Co., Inc New York, N. Y., 1948).
[84] I. Waller and D. R. Hartree, Proc. Roy. Soc. [A] **124**, 119 (1929).
[85] G. Herzog, Z. Physik **69**, 207 (1931); Z. Physik **70**, 583 (1931).
[86] G. Wentzel, Z. Physik **40**, 590 (1927).

WASHINGTON, September 4, 1956.